HHS Public Access

Author manuscript

Brain Behav Immun. Author manuscript; available in PMC 2022 January 01.

Published in final edited form as:

Brain Behav Immun. 2021 January ; 91: 296–314. doi:10.1016/j.bbi.2020.10.008.

Dexmedetomidine attenuates sepsis-associated inflammation and encephalopathy via central α2A adrenoceptor

Bin Mei[1,2], **Jun Li**[1], **Zhiyi Zuo**[1]

[1]Department of Anesthesiology, University of Virginia, Charlottesville, Virginia 22901, U.S.A.

[2]Department of Anesthesiology, First Affiliated Hospital of Anhui Medical University, Hefei City, Anhui Province, P. R. China.

Abstract

Sepsis-associated encephalopathy (SAE) is a significant clinical issue that is associated with increased mortality and cost of health care. Dexmedetomidine, an α2 adrenoceptor agonist that is used to provide sedation, has been shown to induce neuroprotection under various conditions. This study was designed to determine whether dexmedetomidine protects against SAE and whether α2 adrenoceptor plays a role in this protection. Six- to eight-week old CD-1 male mice were subjected to cecal ligation and puncture (CLP). They were treated with intraperitoneal injection of dexmedetomidine in the presence or absence of α2 adrenoceptor antagonists, atipamezole or yohimbine, or an α2A adrenoceptor antagonist, BRL-44408. Hippocampus and blood were harvested for measuring cytokines. Mice were subjected to Barnes maze and fear conditioning 14 days after CLP to evaluate their learning and memory. CLP significantly increased the proinflammatory cytokines including tumor necrosis factor α, interleukin (IL)-6 and IL-1β in the blood and hippocampus. CLP also increased the permeability of blood-brain barrier (BBB) and impaired learning and memory. These CLP detrimental effects were attenuated by dexmedetomidine. Intracerebroventricular application of atipamezole, yohimbine or BRL-44408 blocked the protection of dexmedetomidine on the brain but not on the systemic inflammation. Astrocytes but not microglia expressed α2A adrenoceptors. Microglial depletion did not abolish the protective effects of dexmedetomidine. These results suggest that dexmedetomidine reduces systemic inflammation, neuroinflammation, injury of BBB and cognitive dysfunction in septic mice. The protective effects of dexmedetomidine on the brain may be mediated by α2A adrenoceptors in the astrocytes.

Address correspondence to: Dr. Zhiyi Zuo, Department of Anesthesiology, University of Virginia Health System, 1 Hospital Drive, PO Box 800710, Charlottesville, Virginia 22908-0710. Tel: 434-924-2283, Fax: 434-924-2105, zz3c@virginia.edu.

Authors' contribution: ZZ conceived the concept of the project; BM, JL and ZZ designed the studies; BM and JL performed the experiments. BM performed initial data analysis. BM drafted the manuscript. ZZ performed the final analysis of the data and wrote the manuscript.

Competing interests: The authors declare no competing interests.

Keywords

α2A adrenoceptor; astrocytes; dexmedetomidine; sepsis; sepsis-associated encephalopathy

Introduction

Sepsis is a life-threatening disease with an incidence of 0.3 to 1% per year in the United States (Fleischmann et al., 2016). Sepsis-associated encephalopathy (SAE) is a common and severe complication during and after sepsis, which is associated with increased needs and cost of health care and mortality (Iwashyna et al., 2010; Sonneville et al., 2017). Up to 40% of sepsis survivors have been reported to have long-term cognitive dysfunction after sepsis (Iwashyna et al., 2010; Sprung et al., 1990; Winters et al., 2010). Athough SAE has been a focus of research, clinical methods to avoid and treat SAE are not available.

Neuroinflammation in the central nervous system (CNS) induced by sepsis is considered a potential mechanism of delayed cognitive dysfunction (Xing et al., 2018). Systemic inflammation during sepsis is transmitted into the brain via impaired blood-brain barrier (BBB) (Natale et al., 2019; Obermeier et al., 2013; Subramaniyan and Terrando, 2019). During the process of systemic inflammation, the integrity of BBB was not only challenged by peripheral inflammation but also influenced by the glial cells in the CNS (Haruwaka et al., 2019; Spampinato et al., 2019). The high mobility group box 1 protein (HMGB1) released from activated microglia and astrocytes has been reported to damage the endothelial structure and function via activating receptor for advanced glycation end-products (RAGE) (Faraco et al., 2007; Festoff et al., 2016). Extracellular HMGB1 is considered to be an important late proinflammatory mediator in sepsis. Interventions to inhibit HMGB1 activity and release are being investigated to improve the outcome of diseases with acute and chronic inflammation including sepsis (Wang et al., 2014; Wang et al., 2004).

The highly selective α2 adrenoceptor agonist, dexmedetomidine, is commonly used for patient's sedation in the intensive care unit (ICU). Activating α2 adrenoceptors in locus ceruleus may contribute to the sedative effect (Song et al., 2017; Zhang et al., 2015). Systemic administration of dexmedetomidine can improve neurocognitive functions (Mei et al., 2018; Skrobik et al., 2018) and reduce neuroinflammation after various other conditions including surgery (Hu et al., 2018; Mei et al., 2018; Skrobik et al., 2018; Su et al., 2016; Yin et al., 2019). However, the mechanism for this phenomenon remains unclear. *In vitro* studies have showed that dexmedetomidine modulates the functions of both microglia and astrocytes and that α2 adrenoceptor may mediate these effects (Gao et al., 2019; Liu et al., 2017). Since dexmedetomidine applied peripherally can induce sedation, dexmedetomidine may be able to cross the BBB and confer direct central effect (Song et al., 2017).

With the above information, we hypothesize that dexmedetomidine protects the neurocognitive function against sepsis by inhibiting glial activation, neuroinflammation and BBB damage via activating α2 adrenoceptors in the CNS. These hypotheses were tested in the cecal ligation and puncture (CLP)-induced sepsis model in mice.

Methods

The protocol of animal experiments in this study was approved by the Institutional Animal Care and Use Committee of the University of Virginia (Charlottesville, VA, USA). All animal experiments were conducted in accordance with the National Institutes of Health Guide for the Care and Use of Laboratory Animals (National Institutes of Health publication no. 80–23, revised in 2011).

Groups and experimental protocols

Six- to eight-week old CD-1 male mice were purchased from Charles River Laboratory Inc. (Wilmington, MA, USA). In experiment 1, they were randomly assigned to following three groups: control, sham surgery and sepsis. Control mice did not receive surgery. Mice in the sham group received laparotomy but were without CLP. Mice in the sepsis group had CLP (Fig. 1A).

To test whether dexmedetomidine had a protective effect against sepsis, four groups were included in experiment 2: sham surgery, sepsis, dexmedetomidine plus sham surgery and dexmedetomidine plus sepsis. In dexmedetomidine plus sham surgery and dexmedetomidine plus sepsis groups, dexmedetomidine (Cat. No.: 0409–1638-02; Hospira, Lake Forest, IL, USA) was dissolved in 0.9% saline and intraperitoneally administered at 50 μg/kg every 2 hours for 6 hours with the first injection at 5 min after the onset of CLP (Fig. 1B) (Hu et al., 2018).

To determine the role of α2 adrenoceptors in mediating the neuroprotective effect of dexmedetomidine, the following four groups were included in experiment 3: sepsis, dexmedetomidine plus sepsis, atipamezole (a selective α2 adrenoreceptor antagonist) (Hara et al., 2016) plus dexmedetomidine plus sepsis and atipamezole plus sepsis. Atipamezole (Cat. No.: A9611; Sigma-Aldrich, St. Louis, MO, USA) was dissolved in 5% dimethyl sulfoxide (DMSO; Fisher Scientific, Fair Lawn, NJ, USA) in saline, and intracerebroventricularly injected at 25 nmoles per mouse in atipamezole plus dexmedetomidine plus sepsis and atipamezole plus sepsis groups immediately after the onset of CLP (Stone et al., 1997). The volume (5 μl) of 5% DMSO was intracerebroventricularly administered to mice in sepsis and dexmedetomidine plus sepsis groups. Dexmedetomidine administration was the same as that in experiment 2 (Fig. 1C).

Another α2 adrenoceptor antagonist, yohimbine that has no affinity to imidazoline receptor (Kino et al., 2005), was used in experiment 4 that had 4 groups: sepsis, dexmedetomidine plus sepsis, yohimbine plus dexmedetomidine plus sepsis and yohimbine plus sepsis. Yohimbine hydrochloride (Cat. No.: Y0000656; Sigma-Aldrich, St. Louis, MO, USA) was dissolved in saline and intracerebroventricularly injected at 10 μg/kg (Sierralta et al., 1996). Saline was intracerebroventricularly administered to mice in sepsis and dexmedetomidine plus sepsis groups (Fig. 1C).

To determine whether α2A adrenoceptor mediated dexmedetomidine-induced protection, a selective α2A adrenoceptor antagonist (Hara et al., 2016), BRL-44408 (Cat. No.: B4559; Sigma-Aldrich, St. Louis, MO, USA), was used. Four groups of mice were included in

experiment 5: sepsis, dexmedetomidine plus sepsis, BRL-44408 plus dexmedetomidine plus sepsis and BRL-44408 plus sepsis. BRL-44408 was dissolved in saline and intracerebroventricularly injected at 5 μg/mouse (Wang et al., 2017). Saline was intracerebroventricularly administered to mice in sepsis and dexmedetomidine plus sepsis groups (Fig. 1C).

Experiment 6 was conducted to investigate the involvement of microglia in the effects of dexmedetomidine on septic mice. The following four groups were included: control, PLX3397, PLX3397 plus sepsis and dexmedetomidine plus PLX3397 plus sepsis group. The mice in control and PLX3397 groups did not receive CLP or sham surgery. Mice in PLX3397 plus sepsis and dexmedetomidine plus PLX3397 plus sepsis groups had sepsis. Dexmedetomidine was administered to mice in the same way as that stated above. Mice in PLX3397, PLX3397 plus sepsis and dexmedetomidine plus PLX3397 plus sepsis groups were pretreated with PLX3397 for 14 days, which was reported to be able to deplete microglia in the brain (Liang et al., 2019) (Fig. 1D).

Sepsis model

Sepsis was induced by CLP, a classical model, as we and others previously described (Rittirsch et al., 2009; Xing et al., 2018). Briefly, under anesthesia with 2% isoflurane, the animal was placed on a heating pad (Physitemp Instruments Inc., Clifton, NJ, USA) to maintain body temperature at 37°C. After skin disinfection, a 1-cm abdominal middle-line incision was made to expose the cecum. The cecum was ligated in the middle between distal pole and the base of the cecum to induce moderate sepsis. A single puncture with a 21 G needle through the whole cecum was made between the ligation site and tip of the cecum. A small amount of stool was squeezed out through the puncture site. The cecum was placed back into the abdomen, the peritoneum, fasciae and abdominal musculature were closed with a sterile 6–0 silk suture. The skin was closed by metallic clips. Animals received infiltration of 0.25% bupivacaine to the surgical site. Another skin disinfection was applied after surgery. For animals that received surgeries, 50 ml/kg normal saline was injected subcutaneously. Animals in sham surgery groups underwent the same surgical procedures but without CLP.

Intracerebroventricular injections

As previously described (Sankowski et al., 2019), mice receiving intracerebroventricular injections were anesthetized with 2% isoflurane and placed in a stereotactic head frame in the prone position. The injection site was located as follows: 1.00 mm mediolateral, −0.3 mm anteroposterior and −2.5 mm dorsoventral from bregma. The injection was performed with a 26 G Hamilton syringe needle for 1 min. After the injection, the needle remained in place for 30 s before being removed.

Microglial depletion

The depletion of microglia was achieved with the selective colony stimulating factor-1 receptor (CSF1R) kinase inhibitor Pexidartinib (PLX3397; cat No.: C-1271; Chemgood LLC, VA, USA), which was administered via oral gavage. As previously described (Liang et al., 2019), PLX3397 was prepared by mixing with 5% DMSO, 45% polyethylene glycol

300, and 50% H_2O in sequence. Five-week old CD-1 male mice were administered with the prepared PLX3397 once a day at 46.25 mg/kg for 14 days. An equal volume of vehicle solution but without PLX3397 was administered to the mice in control group.

Behavioral test

The Barnes maze and fear conditioning test were used to determine the cognitive functions of mice.

Two weeks after surgery, mice were subjected to Barnes maze to test their spatial learning and memory. As we describe previously (Liang et al., 2018), mice were placed in the middle of a circular platform with 20 equally spaced holes (SD Instruments, San Diego, CA). One of these holes was connected to a dark chamber called target box. Aversive noise (85 dB) and bright light (200 W) shed on the platform were used to encourage mice to find the target box. They had a spatial acquisition phase that lasted for 4 days with 3 min per trial, 2 trials per day and 15 min between each trial. Animals then went through the reference memory phase on day 1 and day 8 after the training sessions. No test or handling was performed from day 1 to day 8 after the training. The latency to find the target box during each trial was recorded with the assistance of ANY-Maze video tracking system (SD Instruments, San Diego, CA).

One day after Barnes maze test, mice were subjected to a fear conditioning test as we previously described (Liang et al., 2018). Each mouse was placed into a test chamber wiped with 70% alcohol and exposed to 3 tone-foot shock pairings (tone: 2000 Hz, 85 db, 30 s; foot shock: 0.7 mA, 2 s) with an interval of 1 min in a relatively dark room. The mouse was removed from this test chamber 30 s after the conditioning stimuli. The animal was placed back into the same chamber without the tone and shock 24 h later for 6 min. The animal was placed 2 h later into another test chamber that had different context and smell from the first test chamber in a relatively light room. This second chamber was wiped with 1% acetic acid. Freezing behavior was recorded for 3 min without the tone stimulus. The tone was then turned on for 3 cycles, each cycle for 30 s followed by 1-min inter-cycle interval (4.5 min in total). Animal behavior in these two chambers was video recorded. The length of freezing behavior in the 6 min in the first chamber (context-related) and 4.5 min in the second chamber (tone-related) was recorded by an observer who was blind to the group assignment.

Measurement of blood-brain permeability

The BBB permeability was tested by Evans blue (EB) dye as previously described (Kikuchi et al., 2019). EB (2% in saline, 5 ml/kg; Sigma-Aldrich, St. Louis, MO, USA) was injected 24 h after surgery via tail vein. Mice were deeply anesthetized 60 min later and transcardially perfused with saline to remove the intravascular dye. The hippocampus of each mouse was harvested and weighed separately. The hippocampi were homogenized in 1 ml 50% trichloroacetic acid (cat No.: T4885, Sigma-Aldrich, St. Louis, MO, USA), incubated overnight at 4°C, and centrifuged at 13000 g for 30 min. The amount of EB in the supernatant was quantified by spectrophotometer at 620 nm. The results were expressed as micrograms per gram of hippocampus tissue weight.

Immunoblot analysis

Mice were anesthetized deeply by isoflurane 24 h after surgery and transcardially perfused with saline. The hippocampus and kidneys were harvested for Western immunoblotting. Kidneys were used as a positive control for α2 adrenoceptors. Tissues were homogenized in RIPA buffer (Cat. No.: 89901; Thermo Scientific, Worcester, MA, USA) with protease inhibitors (Cat. No.: P2714; Sigma, St. Louis, MO, USA) on ice as described (Xing et al., 2018). Homogenates were centrifuged at 4°C at 13000 g for 25 min and the supernatant was collected for immunoblotting.

Thirty micrograms of total proteins were loaded into each well SDS-PAGE gels (4 – 12%; Bio-Rad Laboratories Inc., Hercules, CA, USA). Proteins were transferred onto a nitrocellulose membrane (Bio-Rad Laboratories Inc., Hercules, CA, USA) and shaken with blocking buffer (Cat. No.: 37573; Thermo Scientific, Logan, UT, USA) for 1 h at room temperature. The membrane was incubated with following primary antibodies under gentle agitation at 4°C overnight: rabbit monoclonal anti-HMGB1 antibody (1:1000, Cat. No.: 6893; Cell Signaling Technology, Danvers, MA, USA), rabbit polyclonal anti-RAGE antibody (1:1000, Cat. No.: ab3611; Abcam, Cambridge, MA, USA), goat polyclonal anti-α2A adrenoceptor antibody (1:500, Cat. No.: ab45871; Abcam), mouse monoclonal anti-α2B adrenoceptor antibody (1:1000, Cat. No.: NBP2–66606; Novus Biologicals), rabbit polyclonal anti-α2B adrenoceptor antibody (1:1000, Cat. No.: PA5–109364; Invitrogen), mouse monoclonal anti-α2C adrenoceptor antibody (1:1000, Cat. No.: ab167433; Abcam), rabbit polyclonal anti-α2C adrenoceptor antibody (1:1000, Cat. No.: NB100–93554; Novus Biologicals) or rabbit polyclonal anti-α-tublin antibody (1:1000, Cat. No.: 2148; Cell Signaling Technology, Danvers, MA, USA). Secondary goat anti-rabbit antibody (1:5000, Cat. No.: 7074S; Cell Signaling Technology, Danvers, MA, USA), mouse anti-goat antibody (1:5000, Cat. No.: sc-2354; Santa Cruz Biotechnology) or recombinant anti-mouse antibody (1:5000, Cat. No.: sc-516102; Santa Cruz Biotechnology) were used. Quantitative analysis of the protein bands was performed using an Image-Quant 5.0 GE Healthcare Densitometer (GE Healthcare, Sunnyvale, CA, USA) after visualization with enhanced chemiluminescence. The results of interested bands were normalized by the corresponding data of α-tublin or β actin from the same samples. The results were then normalized by those of control group or sepsis group. To compare the abundance of α2 adrenoceptor subtypes in tissues, the process to visualize the bands corresponding to these proteins was under identical enhanced chemiluminescent conditions.

Immunofluorescent staining

The microglial staining was performed as we have described before (Xing et al., 2018). Briefly, mice were under deep isoflurane anesthesia and transcardially perfused with 4% paraformaldehyde at 24 h after surgery. Brains were harvested, fixed in 4% paraformaldehyde at 4°C for 24 h and then embedded in paraffin. Coronal sections at 5 μm were mounted on slides. Antigen retrieval was performed in sodium citrate buffer (10 mM sodium citrate, 0.05% Tween 20, pH 6.0) at 95 to 100°C for 20 min. The sections were incubated with 5% normal donkey serum and 1% bovine serum albumin in Tris-buffered saline for 2 h at room temperature and then incubated at 4°C overnight with the rabbit anti-ionized calcium binding adapter molecule 1 (Iba-1) antibody (1:200 dilution, Cat. No.: PA5–

27436; Invitrogen, Eugene, ON, USA). Sections were rinsed in Tris-buffered saline (TBS). The donkey anti-rabbit IgG antibody conjugated with Alexa Fluor 594 (1:200 dilution, Cat. No.: A21207; Invitrogen, Eugene, ON, USA) was chose as the secondary antibody. The sections were incubated with secondary antibody for 1 h at room temperature in the dark.

To investigate whether astrocytes were the source of C3 in hippocampus, sections from sham group and sepsis group were used for glial fibrillary acidic protein (GFAP) and C3 co-staining. Sections were incubated with goat anti-GFAP antibody (1:500 dilution, Cat. No.: ab53554; Abcam) and then with donkey anti-goat IgG antibody conjugated with Alexa Fluor 488 (1:200 dilution, Cat. No.: ab32790, Invitrogen). C3 was identified by rabbit polyclonal anti-C3 antibody (1:200 dilution, Cat. No.: ab11887; Abcam) followed by a donkey anti-rabbit IgG antibody conjugated with Alexa Fluor 594 (1:200 dilution, Cat. No.: ab21207; Invitrogen).

The subtypes of α2 adrenoceptors, α2A, α2B and α2C adrenoceptors, were respectively co-stained with the biomarkers of microglia and astrocytes in mice receiving CLP. Microglia were identified by Iba-1 staining as mentioned above. The rabbit anti-GFAP antibody (1:500 dilution, Cat. No.: ab7260; Abcam, Cambridge, MA, USA) followed by the donkey anti-rabbit IgG antibody conjugated with Alexa Fluor 594 (1:200 dilution, Cat. No.: A21207; Invitrogen, Eugene, ON, USA) was used to identify astrocytes. The goat anti-α2A adrenoceptor antibody (1:50 dilution, Cat. No.: ab45871; Abcam) that was detected by the donkey anti-goat IgG antibody conjugated with Alexa Fluor 488(1:200 dilution, Cat. No.: A32790; Invitrogen) was used to identify α2A adrenoceptors. The mouse anti-α2B adrenoceptor antibody (1:50 dilution, Cat. No.: NBP2–66606; Novus Biologicals) that was detected by the donkey anti-mouse IgG antibody conjugated with Alexa Fluor 488(1:200 dilution, Cat. No.: A21202; Invitrogen) or rabbit polyclonal anti-α2B adrenoceptor antibody (1:50, Cat. No.: PA5–109364; Invitrogen) followed with donkey anti-rabbit IgG antibody conjugated with Alexa Fluor 488 (1:200 dilution, Cat. No.: A21207; Invitrogen) was used to identify α2B adrenoceptors. The mouse anti-α2C adrenoceptor antibody (1:50 dilution, Cat. No.: ab167433; Abcam, Cambridge, MA, USA) that was detected by the donkey anti-mouse IgG antibody conjugated with Alexa Fluor 488 or rabbit polyclonal anti-α2C adrenoceptor antibody (1:1000, Cat. No.: NB100–93554; Novus Biologicals) followed with donkey anti-rabbit IgG antibody conjugated with Alexa Fluor 488 (1:200 dilution, Cat. No.: A21207; Invitrogen) was used to identify α2C adrenoceptor staining.

Images were acquired with a fluorescence microscope with a charge-coupled device camera. A negative control omitting the incubation with the primary antibody was included in all experiments. Three independent microscopic fields in each section were randomly acquired in the DG and CA3 areas. Three sections per mouse were imaged. For quantification of Iba-1 staining in experiments other than microglial deletion experiment, the number of pixels per image with intensity above a predetermined threshold level was measured. The threshold level was the measurement on the area without positive staining of the same brain section. This measurement was performed by using the Image J 1.47n software. The degree of positive immunoreactivity was reflected by the percentage of the positively stained area in the total area of the image (whole microscopic field). The 18 measurements (9 from DG area and 9 from CA3 area) from each mouse were averaged to derive the value for the mouse. To

evaluate the depletion of microglia, the number of Iba-1 positive cells per 500 μM^2 was determined. These two methods (fluorescent staining intensity measurement and cell number counting) were used because determining the fluorescent intensity in an image was easy and quick. However, determining Iba-1 positive cell density was needed to eliminate the introduction of a possible error in evaluating the depletion of microglia by PLX3397 if PLX3397 could decrease the expression of Iba-1 or change the morphology of microglia. To evaluate the degree of GFAP and C3 co-localization, the number of cells positively for both GFAP and C3 per 100 μM^2 was determined. All quantitative analyses were performed in a blinded fashion.

Cytokines determination in serum and hippocampus

Mice were euthanized by deep isoflurane anesthesia at 24 h after surgery. Blood was collected from right ventricle after thoracotomy. After being placed for 2 h at room temperature, blood was centrifuged at 1300 relative centrifugal field for 20 min at 4°C and serum was collected. After blood collection, the bilateral hippocampi were harvested after saline perfusion. The dissection of hippocampus was performed on ice. The concentrations of tumor necrosis factor (TNF)-α, interleukin (IL)-6 and IL-1β in the serum and hippocampus were determined by commercial ELISA kits (R&D SYSTEM). The hippocampal tissue preparation was the same as that for immunoblotting. After supernatant was collected, the concentrations of cytokines were determined. To reflect the activation of astrocytes (Liddelow et al., 2017; Zhao et al., 2020), the complement C3 was measured in the hippocampus by a commercial kit (Cat. No.: ab157711; Abcam, Cambridge, MA, USA). The results of cytokines in serum were expressed as pg/ml. The concentrations of cytokines and complement C3 in the hippocampus were normalized by total protein content and was presented as pg/mg protein.

Statistical analysis

GraphPad prism 8.0 was used to analyze the data. All data are present as Mean ± S.D. Individual data point is presented in the bar figures. The data of training sessions of Barnes tests from various sets of experiments was analysed by two-way repeated measures ANOVA. Shapiro-Wilk test was used to determine the distribution of data. In experiment 1, one-way ANOVA followed with Tukey's multiple comparisons test was used to analyse the data because all data were normally distributed. In experiments 2 to 5, data was analyzed by two-way ANOVA test followed by Tukey's multiple comparisons test. The two factors were sepsis and dexmedetomidine in experiment 2 and dexmedetomidine and an inhibitor (atipamezole, BRL-44408 or Yohimbine) in other experiments. In experiment 6, the results of microglial depletion by PLX3397 were analyzed by a two-tailed unpaired *t* test (comparison of Iba-1 positive cell density between control and PLX3397 treated mice). Other data from this experiment was analyzed by one-way ANOVA test followed by Tukey's multiple comparisons test. Mortality rates were compared by Z-test. A $P < 0.05$ was considered to indicate a statistically significant difference.

Results

Sepsis impaired learning, memory and blood-brain barrier and induced neuroinflammation in mice

As the increase in training sessions, the time needed for mice to identify the target box in Barnes maze was decreased in all groups (Fig. 2A). Sepsis but not sham surgery was a significant factor to influence the performance of mice in the training sessions [F(1,18) = 8.966, P = 0.008 for sepsis to compare with control condition; F(1,18) = 0.809, P = 0.380 for sham surgery to compare with control condition]. Two factors were training sessions and sepsis or training sessions and surgery, respectively, for these two analyses. There was an interaction between training sessions and sepsis [F(3,18) = 4.115, P = 0.011] but there was no interaction between training sessions and sham surgery [F(3,18) = 0.601, P = 0.617]. Sepsis, but not sham surgery, increased the time for mice to identify the target box at one day [14 days after surgery, overall F(2, 27) = 12.62; 13.9 ± 6.4 s in sham surgery group *vs.* 69.5 ± 49.8 s in sepsis group, $P = 0.0006$] and 8 days [21 days after surgery, overall F(2, 27) = 14.72; 15.3 ± 5.1 s in sham surgery group *vs.* 84.5 ± 56.7 s in sepsis group, $P = 0.0002$] after the training sessions. Also, compared with sham surgery, sepsis decreased not only the context-related fear conditioning [overall F(2, 27) = 15.22; 125 ± 30 s in sham surgery group *vs.* 64 ± 23 s in sepsis group, $P = 0.0213$] but also the tone-related fear conditioning [overall F(2, 27) = 17.36; 99 ± 24 s in sham surgery group *vs.* 51 ± 18 s in sepsis group, $P = 0.0061$]. There was no difference in context- and tone-related fear conditioning between control and sham surgery mice (Figs. 2B and 2C). These results suggest that sepsis impairs the learning and memory of mice.

Similar to the behavior data, no significant difference in the expression of HMGB1 and RAGE was found between control group and sham surgery group. Sepsis increased the expressions of HMGB1 [overall F(2, 18) = 17.33; 1.23 ± 0.34 in sham surgery group *vs.* 4.24 ± 1.92 in sepsis group, $P = 0.0003$] and RAGE [overall F(2, 18) = 11.95; 1.71 ± 0.83 in sham surgery group *vs.* 3.63 ± 1.53 in sepsis group, $P = 0.0076$] (Figs. 2D and 2E). A similar pattern of changes occurs in BBB integrity assessed by Evans blue [overall F(2, 15) = 20.75; 33.93 ± 6.48 μg/g in sham surgery group *vs.* 66.88 ± 20.28 μg/g in sepsis group, $P = 0.0010$) (Fig. 2F). These results suggest that sepsis impairs the integrity of BBB in mice.

The expression of Iba-1, a microglial marker, was increased after sepsis [overall F(2, 15) = 116.5; 1.64 ± 0.13% in sham surgery group *vs.* 6.14 ± 0.99% in sepsis group, $P < 0.0001$] (Figs. 3A). Consistent with the idea that complement C3 is an indicator for the activation of astrocytes (Liddelow et al., 2017; Zhao et al., 2020), most of C3 positive staining was co-localized with GFAP staining. The number of C3 positive cells and C3 concentrations were increased after sepsis [C3 concentrations: overall F(2, 15) = 24.78; 756 ± 285 pg/mg protein in sham surgery group *vs.* 1679 ± 382 pg/mg protein in sepsis group, $P < 0.0001$) (Figs. 3B and 3C]. Similarly, the concentration of TNF-α [overall F(2, 15) = 12.39; 35.2 ± 16.1 pg/ml in sham surgery group *vs.* 150.3 ± 81.1 pg/ml in sepsis group, $P = 0.0279$], IL-6 [overall F(2, 15) = 39.83; 30.1 ± 21.5 pg/ml in sham surgery group *vs.* 601.8 ± 225.0 pg/ml in sepsis group, $P < 0.0001$] and IL-1β [overall F(2, 15) = 8.706; 34.3 ± 25.0 pg/mg protein in sham surgery group *vs.* 113.5 ± 65.7 pg/ml in sepsis group, $P = 0.0386$] in serum was increased in

septic mice. The level of TNF-α [overall F(2, 15) = 22.86; 2.118 ± 1.579 pg/mg protein in sham surgery group *vs.* 8.511 ± 3.302 pg/mg protein in sepsis group, $P = 0.0003$], IL-6 [overall F(2, 15) = 14.22; 5.254 ± 4.578 pg/mg protein in sham surgery group *vs.* 18.35 ± 6.868 pg/mg protein in sepsis group, $P = 0.0014$] and IL-1β [overall F(2, 15) = 17.94; 7.031 ± 4.081 pg/mg protein in sham surgery group *vs.* 21.92 ± 7.183 pg/mg protein in sepsis group, $P = 0.0051$] in the hippocampus were increased (Fig. 3D). These results suggest that sepsis induced systemic inflammation and neuroinflammation.

Dexmedetomidine attenuated sepsis-induced neuroinflammation and impairment of learning, memory and integrity of BBB

As shown above, mice improved their performance in the training sessions of Barnes maze tests (Fig. 4A). Dexmedetomidine improved the performance of septic mice [F(1,21) = 14.324, P = 0.001] but not sham surgery mice [F(1,18) = 0.0776, P = 0.3784]. Two factors in the analyses were training sessions and dexmedetomidine. There was no interaction between training sessions and dexmedetomidine in septic mice [F(3,21) = 1.078, P = 0.365] and in sham surgery mice [F(3,21) = 0.228, P = 0.877]. Compared to mice in sepsis group, mice receiving dexmedetomidine needed less time to identify the target box at one day [14 days after surgery, overall F(1, 40) = 7.976 for the analysis of dexmedetomidine as the factor; 59.3 ± 50.9 s in sepsis group *vs.* 22.6 ± 24.6 s in dexmedetomidine plus sepsis group, $P = 0.0250$] and 8 days [21 days after surgery, overall F(1, 40) = 8.365 for the analysis of dexmedetomidine as the factor; 80.0 ± 61.5 s in sepsis group *vs.* 33.7 ± 36.1 s in dexmedetomidine plus sepsis group, $P = 0.0255$] (Fig. 4B). Dexmedetomidine increased the freezing time in the context-related fear conditioning [overall F(1, 40) = 24.68 for the analysis of dexmedetomidine as the factor; 60.3 ± 13.3 s in sepsis group *vs.* 90.9 ± 26.0 s in dexmedetomidine plus sepsis group, $P = 0.0197$] and the tone-related fear conditioning [overall F(1, 40) = 9.750 for the analysis of dexmedetomidine as the factor; 75.5 ± 33.1 s in sepsis group *vs.* 128.9 ± 34.2 s in dexmedetomidine plus sepsis group, $P = 0.0118$] (Fig. 4C). These results suggest that dexmedetomidine attenuated sepsis-induced learning and memory impairment.

Administration of dexmedetomidine alleviated the sepsis-induced increase of HMGB1 [overall F(1, 28) = 5.015 for the analysis of dexmedetomidine as the factor; 1.81 ± 0.96 in sepsis group *vs.* 0.76 ± 0.42 in dexmedetomidine plus sepsis group, $P = 0.0076$] and RAGE [overall F(1, 28) = 5.564 for the analysis of dexmedetomidine as the factor; 1.64 ± 0.52 in sepsis group *vs.* 0.82 ± 0.52 in dexmedetomidine plus sepsis group, $P = 0.0089$] in the hippocampus (Figs. 4D and 4E). Dexmedetomidine also improved the integrity of BBB in septic mice [overall F(1, 36) = 14.940 for the analysis of dexmedetomidine as the factor; 72.98 ± 16.96 μg/g in sepsis group *vs.* 57.43 ± 6.13 μg/g in dexmedetomidine plus sepsis group, $P = 0.0397$] (Fig. 4F). These results suggest that dexmedetomidine maintains the integrity of BBB in septic mice.

With dexmedetomidine administration, the increased expression of Iba-1 [overall F(1, 20) = 412.6 for the analysis of dexmedetomidine as the factor; 6.17 ± 0.21% in sepsis group *vs.* 2.99 ± 0.54 in dexmedetomidine plus sepsis group, $P < 0.0001$] and complement C3 [overall F(1, 20) = 39.88 for the analysis of dexmedetomidine as the factor; 2135 ± 537 pg/mg

protein in sepsis group *vs.* 1118 ± 548 pg/mg protein in dexmedetomidine plus sepsis group, $P = 0.0014$] in the hippocampus of septic mice was reduced (Figs. 5A to 5C). Compared with sepsis group, dexmedetomidine decreased the concentrations of IL-6 [overall F(1, 20) = 180.1 for the analysis of dexmedetomidine as the factor; 694.1 ± 178.7 pg/ml in sepsis group *vs.* 480.5 ± 82.7 pg/ml in dexmedetomidine plus sepsis group, $P = 0.0080$] and IL-1β [overall F(1, 20) = 13.59 for the analysis of dexmedetomidine as the factor; 110.6 ± 64.9 pg/ml in sepsis group *vs.* 34.8 ± 13.8 pg/ml in dexmedetomidine plus sepsis group, $P = 0.0072$] in the serum. For the cytokines in the hippocampus, dexmedetomidine also decreased the increased concentrations of IL-6 [overall F(1, 20) = 10.59 for the analysis of dexmedetomidine as the factor; 14.2 ± 7.8 pg/mg protein in sepsis group *vs.* 5.2 ± 2.0 pg/mg protein in dexmedetomidine plus sepsis group, $P = 0.0077$] and IL-1β [overall F(1, 20) = 17.52 for the analysis of dexmedetomidine as the factor; 21.8 ± 8.4 pg/mg protein in sepsis group *vs.* 10.8 ± 3.3 pg/mg protein in dexmedetomidine plus sepsis group, $P = 0.0033$] induced by sepsis (Fig. 5D). These results indicate that dexmedetomidine attenuated sepsis-induced systemic inflammation and neuroinflammation.

Intracerebroventricular α2 adrenoceptor antagonism attenuated the protection of dexmedetomidine against sepsis-induced neuroinflammation and impairment of learning, memory and integrity of BBB

Although mice in various groups needed less time to identify target box with increased training sessions of Barnes maze test (Fig. 6A), intracerebroventricular injection of atipamezole, a selective α2 adrenoceptor antagonist (Hara et al., 2016), significantly affected the performance of septic mice with dexmedetomidine treatment [$F(1,18) = 9.637$, $P = 0.006$]. Two factors in the analyses were training sessions and atipamezole in dexmedetomidine-treated mice. There was no interaction between training sessions and atipamezole in these mice [$F(3,18) = 0.703$, $P = 0.554$]. For septic mice receiving dexmedetomidine, intracerebroventricular atipamezole increased the time for mice to identify the target box at one day [14 days after surgery, overall F(1, 38) = 8.041 for the analysis of atipamezole as the factor; 17.7 ± 8.1 s in dexmedetomidine plus sepsis group *vs.* 73.8 ± 57.5 s in atipamezole plus dexmedetomidine plus sepsis group, $P = 0.0425$] and 8 days [21 days after surgery, overall F(1, 38) = 7.330 for the analysis of atipamezole as the factor; 19.7 ± 20.2 s in dexmedetomidine plus sepsis group *vs.* 80.2 ± 54.5 s in atipamezole plus dexmedetomidine plus sepsis group, $P = 0.0405$] after the training sessions (Fig. 6B). Intracerebroventricular atipamezole also decreased the freezing behaviour of mice receiving dexmedetomidine not only in context-related [overall F(1, 38) = 7.630 for the analysis of atipamezole as the factor; 112.5 ± 33.3 s in dexmedetomidine plus sepsis group *vs.* 71.0 ± 27.7 s in atipamezole plus dexmedetomidine plus sepsis group, $P = 0.0105$] but also in tone-related [overall F(1, 38) = 8.164 for the analysis of atipamezole as the factor; 94.1 ± 26.3 s in dexmedetomidine plus sepsis group *vs.* 66.2 ± 18.0 s in atipamezole plus dexmedetomidine plus sepsis group, $P = 0.0303$] fear conditioning (Fig. 6C). These results suggest that α2 adrenoceptor mediates the effects of dexmedetomidine on learning and memory in septic mice.

Compared with intracerebroventricular vehicle, intracerebroventricular atipamezole in septic mice receiving dexmedetomidine increased the expression of HMGB1 [overall F(1, 36) =

23.02 for the analysis of atipamezole as the factor; 0.41 ± 0.20 in dexmedetomidine plus sepsis group *vs.* 0.78 ± 0.33 in atipamezole plus dexmedetomidine plus sepsis group, $P = 0.007$] and RAGE [overall F(1, 36) = 6.201 for the analysis of atipamezole as the factor; 0.48 ± 0.19 in dexmedetomidine plus sepsis group *vs.* 1.04 ± 0.48 in atipamezole plus dexmedetomidine plus sepsis group, $P = 0.0278$] (Figs. 6D and 6E). Intracerebroventricular atipamezole also impaired the integrity of BBB in sepsis treated with dexmedetomidine [overall F(1, 24) = 12.62 for the analysis of atipamezole as the factor; 63.24 ± 20.83 μg/g in dexmedetomidine plus sepsis group *vs.* 109.84 ± 21.15 μg/g in atipamezole plus dexmedetomidine plus sepsis group, $P = 0.0060$] (Fig. 6F). These results indicate a role of α2 adrenoceptor in the effects of dexmedetomidine on BBB integrity in septic mice.

In addition, intracerebroventricular atipamezole increased the expression of Iba-1 [overall F(1, 20) = 73.66 for the analysis of atipamezole as the factor; 2.84 ± 0.36% in dexmedetomidine plus sepsis group *vs.* 4.78 ± 0.69% in atipamezole plus dexmedetomidine plus sepsis group, $P = 0.0003$] and complement C3 [overall F(1, 20) = 6.237 for the analysis of atipamezole as the factor; 1016 ± 303 pg/mg protein in dexmedetomidine plus sepsis group *vs.* 1756 ± 312 pg/mg protein in atipamezole plus dexmedetomidine plus sepsis group, $P = 0.0317$] in the brain of mice with sepsis treated with dexmedetomidine (Figs. 7A and 7B). Although intracerebroventricular atipamezole did not affect the concentrations of TNF-α, IL-6 and IL-1β in the serum of septic mice treated with dexmedetomidine, it increased the concentrations of IL-6 [overall F(1, 20) = 22.91 for the analysis of atipamezole as the factor; 3.96 ± 2.37 pg/mg protein in dexmedetomidine plus sepsis group *vs.* 9.03 ± 2.80 pg/mg protein in atipamezole plus dexmedetomidine plus sepsis group, $P = 0.0476$] and IL-1β [overall F(1, 20) = 15.24 for the analysis of atipamezole as the factor; 6.80 ± 3.47 pg/mg protein in dexmedetomidine plus sepsis group *vs.* 13.90 ± 3.73 pg/mg protein in atipamezole plus dexmedetomidine plus sepsis group, $P = 0.045$] in the hippocampus (Fig. 7D). These results suggest that α2 adrenoceptor mediates the effects of dexmedetomidine on neuroinflammation in septic mice.

Similar to the results of atipamezole, intracerebroventricular yohimbine, a selective α2 adrenoceptor antagonist (Kino et al., 2005), significantly influenced the performance of septic mice treated with dexmedetomidine [$F(1,21) = 11.904$, $P = 0.002$]. Two factors in the analyses were training sessions and yohimbine in dexmedetomidine-treated mice. There was an interaction between training sessions and yohimbine in these mice [$F(3,21) = 3.010$, $P = 0.037$] (Fig. 8A). For septic mice receiving dexmedetomidine, intracerebroventricular yohimbine increased the time for mice to identify the target box at one day [14 days after surgery, overall F(1, 43) = 16.0 for the analysis of yohimbine as the factor; 18.4 ± 8.6 s in dexmedetomidine plus sepsis group *vs.* 54.5 ± 34.4 s in yohimbine plus dexmedetomidine plus sepsis group, $P = 0.0201$] and 8 days [21 days after surgery, overall F(1, 43) = 6.335 for the analysis of yohimbine as the factor; 22.1 ± 15.9 s in dexmedetomidine plus sepsis group *vs.* 61.6 ± 31.5 s in yohimbine plus dexmedetomidine plus sepsis group, $P = 0.0228$] after the training sessions (Fig. 8B). Intracerebroventricular yohimbine also decreased the freezing behaviour of mice receiving dexmedetomidine not only in context-related [overall F(1, 43) = 6.470 for the analysis of yohimbine as the factor; 104.1 ± 25.8 s in dexmedetomidine plus sepsis group *vs.* 74.2 ± 20.1 s in yohimbine plus dexmedetomidine plus sepsis group, $P = 0.0056$] but also in tone-related [overall F(1, 43) = 7.476 for the

analysis of yohimbine as the factor; 103.2 ± 24.3 s in dexmedetomidine plus sepsis group *vs.* 64.6 ± 22.0 s in yohimbine plus dexmedetomidine plus sepsis group, $P = 0.0002$] fear conditioning (Fig. 8C). These results, along with the results of experiments using atipamezole, strongly suggest a role of α2 adrenoceptor in the effects of dexmedetomidine on learning and memory in septic mice.

Intracerebroventricular α2A adrenoceptor antagonism attenuated the protection of dexmedetomidine against sepsis-induced neuroinflammation and impairment of learning, memory and integrity of BBB

As above, the time needed for mice to identify the target box was decreased with increased training sessions (Fig. 9A). Intracerebroventricular BRL-44408, a selective α2A adrenoceptor antagonist (Hara et al., 2016), significantly influenced the performance of septic mice treated with dexmedetomidine [$F(1,21) = 28.660$, $P < 0.001$]. Two factors in the analyses were training sessions and BRL-44408 in dexmedetomidine-treated mice. There was no interaction between training sessions and BRL-44408 in these mice [$F(3,21) = 2.711$, $P = 0.052$]. Compared to septic mice receiving dexmedetomidine, intracerebroventricular BRL-44408 increased the time for mice to identify the target box at one day [14 days after surgery, overall $F(1, 41) = 20.53$ for the analysis of BRL-44408 as the factor; 15.0 ± 7.2 s in dexmedetomidine plus sepsis group *vs.* 41.8 ± 22.0 s in BRL-44408 plus dexmedetomidine plus sepsis group, $P = 0.0373$] and 8 days [21 days after surgery, overall $F(1, 41) = 13.96$ for the analysis of BRL-44408 as the factor; 18.5 ± 10.6 s in dexmedetomidine plus sepsis group *vs.* 51.1 ± 22.6 s in BRL-44408 plus dexmedetomidine plus sepsis group, $P = 0.0219$] after training sessions of Barnes maze test. Intracerebroventricular BRL-44408 also decreased the freezing behaviour of septic mice receiving dexmedetomidine in context-related fear conditioning [overall $F(1, 41) = 20.49$ for the analysis of BRL-44408 as the factor; 101.9 ± 33.2 s in dexmedetomidine plus sepsis group *vs.* 62.3 ± 21.6 s in BRL-44408 plus dexmedetomidine plus sepsis group, $P = 0.0033$] (Figs. 9B and 9C). These results suggest that α2A adrenoceptor mediates the effects of dexmedetomidine on learning and memory in septic mice.

Compared with intracerebroventricular vehicle, intracerebroventricular BRL-44408 increased HMGB1 expression in the hippocampus of septic mice receiving dexmedetomidine [overall, $F(1, 20) = 16.50$ for the analysis of BRL-44408 as the factor; 0.31 ± 0.04 in dexmedetomidine plus sepsis group *vs.* 0.65 ± 0.17 in BRL-44408 plus dexmedetomidine plus sepsis group, $P = 0.0288$) (Figs. 9D and 9E]. Intracerebroventricular BRL-44408 also impaired the integrity of BBB of septic mice treated with dexmedetomidine [overall $F(1, 20) = 58.25$ for the analysis of BRL-44408 as the factor; 56.30 ± 21.25 μg/g in dexmedetomidine plus sepsis group *vs.* 100.17 ± 21.40 μg/g in BRL-44408 plus dexmedetomidine plus sepsis group, $P = 0.0331$] (Fig. 9F). These results indicate a role of α2A adrenoceptor in the effects of dexmedetomidine on BBB integrity in septic mice.

The expression of Iba-1 [overall $F(1, 20) = 124.3$ for the analysis of BRL-44408 as the factor; 2.87 ± 0.57% in dexmedetomidine plus sepsis group *vs.* 4.14 ± 0.39% in BRL-44408 plus dexmedetomidine plus sepsis group, $P = 0.0087$] and complement C3 [overall $F(1, 20) = 8.058$ for the analysis of BRL-44408 as the factor; 991 ± 426 pg/mg protein in

dexmedetomidine plus sepsis group *vs.* 1665 ± 383 pg/mg protein in BRL-44408 plus dexmedetomidine plus sepsis group, $P = 0.0375$] in the hippocampus of septic mice treated with dexmedetomidine was increased by intracerebroventricular BRL-44408 (Figs. 10A to 10C). Although intracerebroventricular BRL-44408 did not affect the cytokine concentrations in the serum of septic mice treated with dexmedetomidine, it increased the hippocampal IL-6 [overall $F(1, 20) = 23.12$ for the analysis of BRL-44408 as the factor; 2.99 ± 21.88 pg/mg protein in dexmedetomidine plus sepsis group *vs.* 7.62 ± 2.20 pg/mg protein in BRL-44408 plus dexmedetomidine plus sepsis group, $P = 0.0420$] and IL-1β [overall $F(1, 20) = 28.85$ for the analysis of BRL-44408 as the factor; 4.24 ± 2.38 pg/mg protein in dexmedetomidine plus sepsis group *vs.* 11.23 ± 2.33 pg/mg protein in BRL-44408 plus dexmedetomidine plus sepsis group, $P = 0.0292$] (Fig. 10D). These results suggest that α2A adrenoceptor mediates the effects of dexmedetomidine on systemic inflammation and neuroinflammation in septic mice.

Astrocytic α2A adrenoceptor played a role in dexmedetomidine-induced protection against neuroinflammation in septic mice

There was only α2A adrenoceptor expressed in the hippocampus. The immunostaining of α2A adrenoceptor was co-localized with the staining of GFAP but not with that of Iba-1. There was no positive staining for α2B and α2C adrenoceptors in the hippocampus (Figs. 11A and 11B). These results suggest that hippocampal astrocytes express α2A adrenoceptors. Similarly, there was staining for α2A adrenoceptors but no staining for α2B and α2C adrenoceptors in the intergeniculate leaf, a brain region that is underneath the hippocampus and has a short distance to the lateral ventricle. The α2A adrenoceptor staining in this brain structure was also co-localized with GFAP staining (Fig. 11C). Consistent with the immunofluorescent staining, Western blotting analysis showed that α2A adrenoceptor was the predominant α2 adrenoceptor in the hippocampus (Fig. 11D). The finding of almost none-detectable α2B and α2C adrenoceptors in the hippocampus was not due to the failure of the antibodies because the antibodies for α2B and α2C adrenoceptors detected clear protein bands in kidney samples (Fig. 11E). These results presented in figure 11 were produced by using mouse monoclonal anti-α2B adrenoceptor antibody and mouse monoclonal anti-α2C adrenoceptor antibody. Due to the concerns of specificity and high background binding of these mouse antibodies when they were used in mouse tissues, rabbit polyclonal anti-α2B adrenoceptor antibody and rabbit polyclonal anti-α2C adrenoceptor antibody were used in additional experiments. These antibodies also did not detect any significant amount of α2B and α2C adrenoceptors in the hippocampus by the immunofluorescent staining and Western blotting analysis (Supplemental figure 1).

After mice were treated with PLX3397 for 14 days, the number of cells positively stained with Iba-1 in the hippocampus was reduced markedly (50 ± 7 per 500 μm^2 in control group *vs.* 4 ± 1 per 500 μm^2 in PLX3397 group, $P < 0.0001$) (Fig. 12A), similar to the finding reported before (Liang et al., 2019). Dexmedetomidine reduced the HMGB1 expression in the hippocampus of septic mice with microglial depletion [overall $F(3, 20) = 4.901$; 2.23 ± 1.03 in PLX3397 plus sepsis group *vs.* 1.45 ± 0.54 in dexmedetomidine plus PLX3397 plus sepsis group, $P = 0.0006$] (Fig. 12B). Dexmedetomidine also reduced the levels of IL-6 [overall $F(3, 20) = 67.11$; 577.4 ± 142.5 pg/ml in PLX3397 plus sepsis group *vs.* 396.5 ±

84.7 pg/ml in dexmedetomidine plus PLX3397 plus sepsis group, $P = 0.0065$] and IL-1β [overall F(3, 20) = 75.37; 89.1 ± 19.7 pg/ml in PLX3397 plus sepsis group *vs.* 64.4 ± 10.7 pg/ml in dexmedetomidine plus PLX3397 plus sepsis group, $P = 0.0196$] in the serum (Fig. 12C). The concentrations of IL-6 [overall F(3, 20) = 16.33; 8.63 ± 142.5 pg/mg protein in PLX3397 plus sepsis group *vs.* 5.03 ± 1.44 pg/mg protein in dexmedetomidine plus PLX3397 plus sepsis group, $P = 0.0085$] and IL-1β [overall F(3, 20) = 20.69; 6.54 ± 2.03 pg/mg protein in PLX3397 plus sepsis group *vs.* 3.84 ± 1.33 pg/mg protein in dexmedetomidine plus PLX3397 plus sepsis group, $P = 0.0115$] in the hippocampus of these mice were also decreased by dexmedetomidine. The release of C3 in the hippocampus of septic mice with microglial depletion was inhibited by dexmedetomidine [overall F(3, 20) = 24.10; 2254 ± 343 pg/mg protein in PLX3397 plus sepsis group *vs.* 1591 ± 403 pg/mg protein in dexmedetomidine plus PLX3397 plus sepsis group, $P = 0.0187$) (Fig. 12C]. These results suggest that dexmedetomidine remains effective in inhibiting neuroinflammation in microglial depletion mice. Unfortunately, the behavior test was not conducted to the microglial depletion mice due to the high mortality (93.3%, 28 mice in total 30 mice) by 3 days after the onset of sepsis. The corresponding mortality of PLX3397 plus dexmedetomidine group was 66.7% (20 mice in total 30 mice). These mortality rates were higher than those of mice without microglial depletion that survived till the end of behaviour testing (21 days after CLP) [37.7% (death: 35 mice in total 93 mice) for sepsis group from experiment 1 to experiment 5, $P < 0.001$ compared with PLX3397 plus sepsis; 33.3% (death: 22 mice in total 66 mice) for sepsis plus dexmedetomidine group from experiment 2 to experiment 5, $P = 0.005$ compared with PLX3397 plus sepsis plus dexmedetomidine].

Discussion

In this study, we used CLP, a classical sepsis animal model. Consistent with our previous findings, CLP induced SAE and inflammation (Xing et al., 2018). Associated with these phenomena, the integrity of BBB was impaired and the factors, HMGB1 and RAGE that are known to regulate the integrity of BBB (Faraco et al., 2007; Festoff et al., 2016), were increased. These sepsis-induced changes were attenuated by dexmedetomidine, suggesting that dexmedetomidine has a protective role in sepsis.

The damage to BBB by systemic inflammation was considered as an initial and important process for the development of SAE (Haileselassie et al., 2020). The increased permeability of BBB allowed peripheral proinflammatory cytokines transmitted into the CNS (Danielski et al., 2018; Kuperberg and Wadgaonkar, 2017). In addition to the direct neuron injury effect, these cytokines activate resting glia (Colonna and Butovsky, 2017). Of note, SAE with glial activation can occur in the absence of obvious BBB damage in rats after CLP (Griton et al., 2020). HMGB1 released from activated astrocyte and microglia induces oxidative stress in the vascular endothelial cells via activating RAGE. Thus, they aggravated the injury of BBB induced by systemic inflammation (He et al., 2012; Okuma et al., 2012). In our study, the levels of proinflammatory cytokines (TNF-a, IL-6 and IL-1β) in the serum was increased after CLP. Astrocytes and microglia may be activated as indicated by increased Iba-1 and C3. HMGB1 and RAGE in the hippocampus were increased. The permeability of BBB in the hippocampus was also increased after CLP. These complex processes may contribute to the significant neuroinflammation in mice with CLP.

Our previous studies have shown that the neuroinflammation can lead to neurocognitive dysfunction (Cao et al., 2012; Xing et al., 2018; Zheng et al., 2017). However, mice with sham surgery in this study did not show learning and memory impairment. These mice also did not have significant systemic inflammation and neuroinflammation. Several studies have shown that exploratory laparotomy under isoflurane anesthesia induces neurocognitive dysfunction via neuroinflammation in elderly mice (Qiu et al., 2016; Qiu et al., 2020). The reasons for these different findings are not known, different ages, surgical details and strains of mice may contribute to this difference. In our study, adult CD-1 mice were used. Elderly C57BL/6 mice were used in those previous studies (Colonna and Butovsky, 2017; He et al., 2012).

Dexmedetomidine has been used clinically to provide sedation. Its neuroprotective effects have been recognized for many years (Ren et al., 2016). In recent years, dexmedetomidine is shown to have a beneficial effect on neurocognitive function (Hu et al., 2018; Mei et al., 2018; Skrobik et al., 2018; Su et al., 2016). In addition to the sedative effect, dexmedetomidine may be anti-inflammatory, which is considered as a potential mechanism for its cognition protective effect (Wang et al., 2019a). Results from another study showed that peripheral application of dexmedetomidine inhibited neuroinflammation after lipopolysaccharide application (Liu et al., 2017). A recent study demonstrated that dexmedetomidine prevented cognitive decline and BBB impairment induced by exogenous administration of HMGB1 (Hu et al., 2018). In addition, dexmedetomidine is shown to reduce CLP-induced learning and memory impairment in rats (Yin et al., 2019). Our study showed that the systemic inflammation and neuroinflammation induced by CLP were reduced by dexmedetomidine. Dexmedetomidine maintained neurocognitive functions and the integrity of BBB. These results clearly suggest the protective role of dexmedetomidine in sepsis.

The mechanism for dexmedetomidine to provide neuroprotection is not fully understood. Previous studies have used α2 adrenoceptor antagonists via systemic routes to implicate a role of α2 adrenoceptor in the effects of dexmedetomidine on the brain (Hu et al., 2018; Sun et al., 2019). It is possible that dexmedetomidine can inhibit systemic inflammation to protect the brain. As found by others (Dardalas et al., 2019) and results from this study, dexmedetomidine reduced the level of proinflammatory cytokines in the blood, which is a critical factor to damage the integrity of BBB and induce neuroinflammation (Wang et al., 2019b). Dexmedetomidine may have a direct effect on neuroinflammation. As a highly selective α2 adrenoceptor agonist, the sedative effect of dexmedetomidine is achieved by activating α2 adrenoceptor in the locus ceruleus (Faraco et al., 2007; Zhang et al., 2015). It is important to note that norepinephrine from locus ceruleus modulates glial function (Qiu et al., 2016), indicating that the adrenergic system in the CNS may influence neuroinflammation induced by various insults. Dexmedetomidine can inhibit the activation of cultured microglia or astrocytes (Gao et al., 2019; Hu et al., 2018; Peng et al., 2013). In this study, intracerebroventricular application of atipamezole blocked dexmedetomidine-induced inhibition on neuroinflammation, the expression of HMGB1 and RAGE in the hippocampus and impairment of BBB in mice with sepsis. The protection of dexmedetomidine on neurocognitive function was also blocked by intracerebroventricular atipamezole. Since intracerebroventricular atipamezole did not affect dexmedetomidine-

induced attenuation of increased cytokines in the blood, these results provide initial evidence that the α2 adrenoceptor in the CNS plays a key role in the neuroprotective effect of dexmedetomidine. In supporting this possibility, yohimbine, another α2 adrenoceptor antagonist given intracerebroventricularly, blocked dexmedetomidine-induced improvement in learning and memory of septic mice.

There are three subtypes of α2 adrenoreceptor: α2A, α2B and α2C (Schwinghammer et al., 2020). α2A adrenoceptor was the only subtype identified in the hippocampus and intergeniculate leaf. These α2A adrenoceptors were expressed in astrocytes and were not found in microglia. Western blotting analysis detected hardly any α2B and α2C adrenoceptors in the hippocampus but detected these two subtypes of adrenoceptors in the kidneys, suggesting the effectiveness of the antibodies in detecting these receptors. No identifiable amount of α2B and α2C adrenoceptors was detected in the hippocampus by mouse monoclonal antibody or rabbit polyclonal antibody. Previous studies using radioligand labelling or general α2 adrenoceptor agonist coupled with using α2C adrenoceptor overexpression or knockout mice have shown the expression of α2C adrenoceptors in the hippocampus of wild-type mice, although α2A adrenoceptor expression is much higher than α2C adrenoceptor expression also in these previous studies (Holmberg et al., 2003; Scheibner et al., 2001). The reasons for different findings on α2C adrenoceptor expression between our study and previous studies are not known but different mouse strains were used (CD-1 mice in our study versus FVB/N and NMRI mice in previous studies). Our results on α2 adrenoceptor expression only in astrocytes are different from previous *in vitro* studies that showed that mRNA encoding α2A adrenoceptor was expressed in microglia activated by lipopolysaccharide (Gyoneva and Traynelis, 2013; Mori et al., 2002). Dexmedetomidine was shown to exhibit direct modulation on the lipopolysaccharide-stimulated microglia *in vitro* but α2 adrenoceptor expression was not determined (Peng et al., 2013). However, the expression of adrenoceptors in microglia was experimental condition-dependent (Gyoneva and Traynelis, 2013). The detection of α2 adrenoceptor protein in our study was in mice with CLP-induced sepsis.

To determine whether α2A adrenoceptor play a role in the neuroprotective effect of dexmedetomidine, BRL-44408, a selective α2A adrenoceptor antagonist (Liu et al., 2017), was used. Similar to the finding with using atipamezole, intracerebroventricular application of BRL-44408 alleviated the inhibition of dexmedetomidine on complement C3 expression in the hippocampus, indicating that the activation of α2A adrenoceptor by dexmedetomidine inhibits the transformation of astrocytes into A1 type. A1 reactive astrocytes are known to produce complement components and release toxic factors, which injure neurons (Clarke et al., 2018). Also, astrocytes can modulate microglial function (Shi et al., 2020). In a mouse Alzheimer's model, activated astrocyte-derived complement C3 activates microglia (Lian et al., 2016). In our study, the inhibition of dexmedetomidine on microglial activation as reflected by Iba-1 expression was reversed by intracerebroventricular BRL-44408. Thus, activating astrocytic α2A adrenoceptor not only reduces the potential injury effects of reactive astrocytes but also contributed to reducing microglial activation, As expected, dexmedetomidine-induced inhibition of proinflammation cytokine expression in the brain, maintenance of BBB integrity and improvement of learning and memory in septic mice were blocked by intracerebroventricular BRL-44408. These results suggest a critical role of

astrocytic α2A adrenoceptor in dexmedetomidine-induced neuroprotective effect. In strongly supporting this suggestion, depleting microglia in the brain did not block the effects of dexmedetomidine on the expression of HMGB1, RAGE and proinflammatory cytokines in the brain, suggesting that the targeting proteins for dexmedetomidine are in astrocytes. A method of astrocytic depletion has been reported (Allnoch et al., 2019). We have not used the method to further imply the role of astrocytes in the dexmedetomidine effects on the brain because it appears that more than half of the GFAP positive cells survive with this method (Allnoch et al., 2019).

Of note, dexmedetomidine has an imidazoline ring structure and has been reported to activate the imidazoline receptor (Khan et al., 1999). In addition to the antagonist activity on α2 adrenoreceptor, atipamezole was reported to have the ability to block imidazoline receptor (Hu et al., 2018). Nevertheless, BRL-44408 does not appear to affect imidazoline receptor (Cobos-Puc et al., 2016). Yohimbine does not have affinity to the imidazoline receptor (Kino et al., 2005). Both Yohimbine and BRL-44408 attenuated the beneficial effects of dexmedetomidine in septic mice. Thus, the role of imidazoline receptor in mediating the protective effects of dexmedetomidine in septic mice is unlikely. However, in contrast to the protective role of α2 adrenoceptor in sepsis as shown in many studies including our study with using dexmedetomidine (Hu et al., 2018; Mei et al., 2018; Skrobik et al., 2018; Su et al., 2016), one study has shown that intravenous BRL-44408 improved survival of septic rats (Miksa et al., 2009). The reason for this different finding is not clear but different species (mice vs. rats) and outcome parameters (survival vs. brain function and structure) are noted between the previous study and our study.

Our findings have significant implications. SAE is a significant clinical issue. Dexmedetomidine has been used clinically. If the protective effects of dexmedetomidine on SAE are confirmed in humans, translation of our findings into clinical practice may be easy. Also, our study provides initial evidence for the protective effects of astrocytic α2A adrenoceptor. Very selective α2A adrenoceptor agonists may be developed to provide protection and have limited side effects.

Our study has limitations. Our results indicate a role of α2A adrenoceptor in the protective effects of dexmedetomidine. However, the downstream mechanisms for this role are not investigated. Our results showed that dexmedetomidine can inhibit systemic inflammation. We have not determined the mechanisms for this inhibition. A very recent study showed that dexmedetomidine promotes the transformation of peripheral macrophages to M2 polarization after liver ischemia (Zhou et al., 2020), which may be a mechanism for dexmedetomidine to inhibit systemic inflammation. Finally, our findings are from animal research and shall not be extrapolated directly to humans.

Conclusion

Our results have shown that sepsis induces a massive systemic inflammation, neuroinflammation, leakage of BBB and the impaired neurocognitive function. Systemic administration of dexmedetomidine attenuated these septic effects. The neuroprotective effects of dexmedetomidine may be mediated by α2A adrenoceptors in astrocytes.

Supplementary Material

Refer to Web version on PubMed Central for supplementary material.

Acknowledgments

Funding: This study was supported by grants (R01 NS099118, R01 HD089999 and RF1 AG061047 to Z Zuo) from the National Institutes of Health, Bethesda, MD, the Robert M. Epstein Professorship endowment (to Z Zuo), University of Virginia, Charlottesville, VA.

References

Allnoch L, Baumgartner W, Hansmann F, 2019 Impact of Astrocyte Depletion upon Inflammation and Demyelination in a Murine Animal Model of Multiple Sclerosis. Int J Mol Sci 20 (16),

Cao L, Li L, Lin D, Zuo Z, 2012 Isoflurane induces learning impairment that is mediated by interleukin 1beta in rodents. PLoS ONE 7 (12), e51431. [PubMed: 23251531]

Clarke LE, Liddelow SA, Chakraborty C, Munch AE, Heiman M, Barres BA, 2018 Normal aging induces A1-like astrocyte reactivity. PNAS 115 (8), E1896–E1905. [PubMed: 29437957]

Cobos-Puc LE, Aguayo-Morales H, Silva-Belmares Y, Gonzalez-Zavala MA, Centurion D, 2016 alpha2A-adrenoceptors, but not nitric oxide, mediate the peripheral cardiac sympatho-inhibition of moxonidine. Eur J Pharmacol 782 35–43. [PubMed: 27112661]

Colonna M, Butovsky O, 2017 Microglia Function in the Central Nervous System During Health and Neurodegeneration. Annu Rev Immunol 35 441–468. [PubMed: 28226226]

Danielski LG, Giustina AD, Badawy M, Barichello T, Quevedo J, Dal-Pizzol F, et al., 2018 Brain Barrier Breakdown as a Cause and Consequence of Neuroinflammation in Sepsis. Mol Neurobiol 55 (2), 1045–1053. [PubMed: 28092082]

Dardalas I, Stamoula E, Rigopoulos P, Malliou F, Tsaousi G, Aidoni Z, et al., 2019 Dexmedetomidine effects in different experimental sepsis in vivo models. Eur J Pharmacol 856 172401. [PubMed: 31108055]

Faraco G, Fossati S, Bianchi ME, Patrone M, Pedrazzi M, Sparatore B, et al., 2007 High mobility group box 1 protein is released by neural cells upon different stresses and worsens ischemic neurodegeneration in vitro and in vivo. J Neurochem 103 (2), 590–603. [PubMed: 17666052]

Festoff BW, Sajja RK, van Dreden P, Cucullo L, 2016 HMGB1 and thrombin mediate the blood-brain barrier dysfunction acting as biomarkers of neuroinflammation and progression to neurodegeneration in Alzheimer's disease. J Neuroinflammation 13 (1), 194. [PubMed: 27553758]

Fleischmann C, Scherag A, Adhikari NK, Hartog CS, Tsaganos T, Schlattmann P, et al., 2016 Assessment of Global Incidence and Mortality of Hospital-treated Sepsis. Current Estimates and Limitations. Am J Respir Crit Care Med 193 (3), 259–72. [PubMed: 26414292]

Gao J, Sun Z, Xiao Z, Du Q, Niu X, Wang G, et al., 2019 Dexmedetomidine modulates neuroinflammation and improves outcome via alpha2-adrenergic receptor signaling after rat spinal cord injury. Br J Anaesth 123 (6), 827–838. [PubMed: 31623841]

Griton M, Dhaya I, Nicolas R, Raffard G, Periot O, Hiba B, et al., 2020 Experimental sepsis-associated encephalopathy is accompanied by altered cerebral blood perfusion and water diffusion and related to changes in cyclooxygenase-2 expression and glial cell morphology but not to blood-brain barrier breakdown. Brain Behav Immun 83 200–213. [PubMed: 31622656]

Gyoneva S, Traynelis SF, 2013 Norepinephrine modulates the motility of resting and activated microglia via different adrenergic receptors. J Biol Chem 288 (21), 15291–302. [PubMed: 23548902]

Haileselassie B, Joshi AU, Minhas PS, Mukherjee R, Andreasson KI, Mochly-Rosen D, 2020 Mitochondrial dysfunction mediated through dynamin-related protein 1 (Drp1) propagates impairment in blood brain barrier in septic encephalopathy. J Neuroinflammation 17 (1), 36. [PubMed: 31987040]

Hara M, Zhou ZY, Hemmings HC Jr., 2016 alpha2-Adrenergic Receptor and Isoflurane Modulation of Presynaptic Ca2+ Influx and Exocytosis in Hippocampal Neurons. Anesthesiology 125 (3), 535–46. [PubMed: 27337223]

Haruwaka K, Ikegami A, Tachibana Y, Ohno N, Konishi H, Hashimoto A, et al., 2019 Dual microglia effects on blood brain barrier permeability induced by systemic inflammation. Nat Commun 10 (1), 5816. [PubMed: 31862977]

He HJ, Wang Y, Le Y, Duan KM, Yan XB, Liao Q, et al., 2012 Surgery upregulates high mobility group box-1 and disrupts the blood-brain barrier causing cognitive dysfunction in aged rats. CNS Neurosci Ther 18 (12), 994–1002. [PubMed: 23078219]

Holmberg M, Fagerholm V, Scheinin M, 2003 Regional distribution of alpha(2C)-adrenoceptors in brain and spinal cord of control mice and transgenic mice overexpressing the alpha(2C)-subtype: an autoradiographic study with [(3)H]RX821002 and [(3)H]rauwolscine. Neurosci 117 (4), 875–98.

Hu J, Vacas S, Feng X, Lutrin D, Uchida Y, Lai IK, et al., 2018 Dexmedetomidine Prevents Cognitive Decline by Enhancing Resolution of High Mobility Group Box 1 Protein-induced Inflammation through a Vagomimetic Action in Mice. Anesthesiology 128 (5), 921–931. [PubMed: 29252509]

Iwashyna TJ, Ely EW, Smith DM, Langa KM, 2010 Long-term cognitive impairment and functional disability among survivors of severe sepsis. JAMA 304 (16), 1787–94. [PubMed: 20978258]

Khan ZP, Ferguson CN, Jones RM, 1999 alpha-2 and imidazoline receptor agonists. Their pharmacology and therapeutic role. Anaesthesia 54 (2), 146–65. [PubMed: 10215710]

Kikuchi DS, Campos ACP, Qu H, Forrester SJ, Pagano RL, Lassegue B, et al., 2019 Poldip2 mediates blood-brain barrier disruption in a model of sepsis-associated encephalopathy. J Neuroinflammation 16 (1), 241. [PubMed: 31779628]

Kino Y, Tanabe M, Honda M, Ono H, 2005 Involvement of supraspinal imidazoline receptors and descending monoaminergic pathways in tizanidine-induced inhibition of rat spinal reflexes. J Pharmacol Sci 99 (1), 52–60. [PubMed: 16127244]

Kuperberg SJ, Wadgaonkar R, 2017 Sepsis-Associated Encephalopathy: The Blood-Brain Barrier and the Sphingolipid Rheostat. Front Immunol 8 597. [PubMed: 28670310]

Lian H, Litvinchuk A, Chiang AC, Aithmitti N, Jankowsky JL, Zheng H, 2016 Astrocyte-Microglia Cross Talk through Complement Activation Modulates Amyloid Pathology in Mouse Models of Alzheimer's Disease. J Neurosci 36 (2), 577–89. [PubMed: 26758846]

Liang P, Shan W, Zuo Z, 2018 Perioperative use of cefazolin ameliorates postoperative cognitive dysfunction but induces gut inflammation in mice. J Neuroinflammation 15 (1), 235. [PubMed: 30134985]

Liang YJ, Feng SY, Qi YP, Li K, Jin ZR, Jing HB, et al., 2019 Contribution of microglial reaction to increased nociceptive responses in high-fat-diet (HFD)-induced obesity in male mice. Brain Behav Immun 80 777–792. [PubMed: 31108168]

Liddelow SA, Guttenplan KA, Clarke LE, Bennett FC, Bohlen CJ, Schirmer L, et al., 2017 Neurotoxic reactive astrocytes are induced by activated microglia. Nature 541 (7638), 481–487. [PubMed: 28099414]

Liu H, Davis JR, Wu ZL, Faez Abdelgawad A, 2017 Dexmedetomidine Attenuates Lipopolysaccharide Induced MCP-1 Expression in Primary Astrocyte. Biomed Res Int 2017 6352159. [PubMed: 28286770]

Mei B, Meng G, Xu G, Cheng X, Chen S, Zhang Y, et al., 2018 Intraoperative Sedation With Dexmedetomidine is Superior to Propofol for Elderly Patients Undergoing Hip Arthroplasty: A Prospective Randomized Controlled Study. Clin J Pain 34 (9), 811–817. [PubMed: 29528863]

Miksa M, Das P, Zhou M, Wu R, Dong W, Ji Y, et al., 2009 Pivotal role of the alpha(2A)-adrenoceptor in producing inflammation and organ injury in a rat model of sepsis. PLoS ONE 4 (5), e5504. [PubMed: 19430535]

Mori K, Ozaki E, Zhang B, Yang L, Yokoyama A, Takeda I, et al., 2002 Effects of norepinephrine on rat cultured microglial cells that express alpha1, alpha2, beta1 and beta2 adrenergic receptors. Neuropharmacol 43 (6), 1026–34.

Natale G, Biagioni F, Busceti CL, Gambardella S, Limanaqi F, Fornai F, 2019 TREM Receptors Connecting Bowel Inflammation to Neurodegenerative Disorders. Cells 8 (10),

Obermeier B, Daneman R, Ransohoff RM, 2013 Development, maintenance and disruption of the blood-brain barrier. Nat Med 19 (12), 1584–96. [PubMed: 24309662]

Okuma Y, Liu K, Wake H, Zhang J, Maruo T, Date I, et al., 2012 Anti-high mobility group box-1 antibody therapy for traumatic brain injury. Ann Neurol 72 (3), 373–84. [PubMed: 22915134]

Peng M, Wang YL, Wang CY, Chen C, 2013 Dexmedetomidine attenuates lipopolysaccharide-induced proinflammatory response in primary microglia. J Surg Res 179 (1), e219–25. [PubMed: 22683080]

Qiu LL, Ji MH, Zhang H, Yang JJ, Sun XR, Tang H, et al., 2016 NADPH oxidase 2-derived reactive oxygen species in the hippocampus might contribute to microglial activation in postoperative cognitive dysfunction in aged mice. Brain Behav Immun 51 109–18. [PubMed: 26254234]

Qiu LL, Pan W, Luo D, Zhang GF, Zhou ZQ, Sun XY, et al., 2020 Dysregulation of BDNF/TrkB signaling mediated by NMDAR/Ca(2+)/calpain might contribute to postoperative cognitive dysfunction in aging mice. J Neuroinflammation 17 (1), 23. [PubMed: 31948437]

Ren X, Ma H, Zuo Z, 2016 Dexmedetomidine Postconditioning Reduces Brain Injury after Brain Hypoxia-Ischemia in Neonatal Rats. J Neuroimmune Pharmacol 11 (2), 238–47. [PubMed: 26932203]

Rittirsch D, Huber-Lang MS, Flierl MA, Ward PA, 2009 Immunodesign of experimental sepsis by cecal ligation and puncture. Nat Prot 4 (1), 31–6.

Sankowski R, Strohl JJ, Huerta TS, Nasiri E, Mazzarello AN, D'Abramo C, et al., 2019 Endogenous retroviruses are associated with hippocampus-based memory impairment. PNAS 116 (51), 25982–25990. [PubMed: 31792184]

Scheibner J, Trendelenburg AU, Hein L, Starke K, 2001 Alpha2-adrenoceptors modulating neuronal serotonin release: a study in alpha2-adrenoceptor subtype-deficient mice. Br J Pharmacol 132 (4), 925–33. [PubMed: 11181434]

Schwinghammer UA, Melkonyan MM, Hunanyan L, Tremmel R, Weiskirchen R, Borkham-Kamphorst E, et al., 2020 alpha2-Adrenergic Receptor in Liver Fibrosis: Implications for the Adrenoblocker Mesedin. Cells 9 (2),

Shi SX, Li YJ, Shi K, Wood K, Ducruet AF, Liu Q, 2020 IL (Interleukin)-15 Bridges Astrocyte-Microglia Crosstalk and Exacerbates Brain Injury Following Intracerebral Hemorrhage. Stroke 51 (3), 967–974. [PubMed: 32019481]

Sierralta F, Naquira D, Pinardi G, Miranda HF, 1996 alpha-Adrenoceptor and opioid receptor modulation of clonidine-induced antinociception. Br J Pharmacol 119 (3), 551–4. [PubMed: 8894177]

Skrobik Y, Duprey MS, Hill NS, Devlin JW, 2018 Low-Dose Nocturnal Dexmedetomidine Prevents ICU Delirium. A Randomized, Placebo-controlled Trial. Am J Respir Crit Care Med 197 (9), 1147–1156. [PubMed: 29498534]

Song AH, Kucyi A, Napadow V, Brown EN, Loggia ML, Akeju O, 2017 Pharmacological Modulation of Noradrenergic Arousal Circuitry Disrupts Functional Connectivity of the Locus Ceruleus in Humans. J Neurosci 37 (29), 6938–6945. [PubMed: 28626012]

Sonneville R, de Montmollin E, Poujade J, Garrouste-Orgeas M, Souweine B, Darmon M, et al., 2017 Potentially modifiable factors contributing to sepsis-associated encephalopathy. Intensive Care Med 43 (8), 1075–1084. [PubMed: 28466149]

Spampinato SF, Bortolotto V, Canonico PL, Sortino MA, Grilli M, 2019 Astrocyte-Derived Paracrine Signals: Relevance for Neurogenic Niche Regulation and Blood-Brain Barrier Integrity. Front Pharmacol 10 1346. [PubMed: 31824311]

Sprung CL, Peduzzi PN, Shatney CH, Schein RM, Wilson MF, Sheagren JN, et al., 1990 Impact of encephalopathy on mortality in the sepsis syndrome. The Veterans Administration Systemic Sepsis Cooperative Study Group. Crit Care Med 18 (8), 801–6. [PubMed: 2379391]

Stone EA, Zhang Y, Hiller JM, Simon EJ, Hillman DE, 1997 Activation of fos in mouse amygdala by local infusion of norepinephrine or atipamezole. Brain Res 778 (1), 1–5. [PubMed: 9462871]

Su X, Meng ZT, Wu XH, Cui F, Li HL, Wang DX, et al., 2016 Dexmedetomidine for prevention of delirium in elderly patients after non-cardiac surgery: a randomised, double-blind, placebo-controlled trial. Lancet 388 1893–1902. [PubMed: 27542303]

Subramaniyan S, Terrando N, 2019 Neuroinflammation and Perioperative Neurocognitive Disorders. Anesth Analg 128 (4), 781–788. [PubMed: 30883423]

Sun YB, Zhao H, Mu DL, Zhang W, Cui J, Wu L, et al., 2019 Dexmedetomidine inhibits astrocyte pyroptosis and subsequently protects the brain in in vitro and in vivo models of sepsis. Cell Death Dis 10 (3), 167. [PubMed: 30778043]

Wang H, Ward MF, Sama AE, 2014 Targeting HMGB1 in the treatment of sepsis. Expert Opin Ther Targets 18 (3), 257–68. [PubMed: 24392842]

Wang H, Yang H, Tracey KJ, 2004 Extracellular role of HMGB1 in inflammation and sepsis. J Intern Med 255 (3), 320–31. [PubMed: 14871456]

Wang K, Wu M, Xu J, Wu C, Zhang B, Wang G, et al., 2019a Effects of dexmedetomidine on perioperative stress, inflammation, and immune function: systematic review and meta-analysis. Br J Anaesth 123 (6), 777–794. [PubMed: 31668347]

Wang RP, Ho YS, Leung WK, Goto T, Chang RC, 2019b Systemic inflammation linking chronic periodontitis to cognitive decline. Brain Behav Immun 81 63–73. [PubMed: 31279681]

Wang YJ, Zuo ZX, Wu C, Liu L, Feng ZH, Li XY, 2017 Cingulate Alpha-2A Adrenoceptors Mediate the Effects of Clonidine on Spontaneous Pain Induced by Peripheral Nerve Injury. Front Mol Neurosci 10 289. [PubMed: 28955200]

Winters BD, Eberlein M, Leung J, Needham DM, Pronovost PJ, Sevransky JE, 2010 Long-term mortality and quality of life in sepsis: a systematic review. Crit Care Med 38 (5), 1276–83. [PubMed: 20308885]

Xing W, Huang P, Lu Y, Zeng W, Zuo Z, 2018 Amantadine attenuates sepsis-induced cognitive dysfunction possibly not through inhibiting toll-like receptor 2. J Mol Med (Berl) 96 (5), 391–402. [PubMed: 29502203]

Yin L, Chen X, Ji H, Gao S, 2019 Dexmedetomidine protects against sepsisassociated encephalopathy through Hsp90/AKT signaling. Mol Med Rep 20 (5), 4731–4740. [PubMed: 31702043]

Zhang Z, Ferretti V, Guntan I, Moro A, Steinberg EA, Ye Z, et al., 2015 Neuronal ensembles sufficient for recovery sleep and the sedative actions of alpha2 adrenergic agonists. Nat Neurosci 18 (4), 553–561. [PubMed: 25706476]

Zhao Y, Yamasaki R, Yamaguchi H, Nagata S, Une H, Cui Y, et al., 2020 Oligodendroglial connexin 47 regulates neuroinflammation upon autoimmune demyelination in a novel mouse model of multiple sclerosis. PNAS 117 (4), 2160–2169. [PubMed: 31932428]

Zheng B, Lai R, Li J, Zuo Z, 2017 Critical role of P2X7 receptors in the neuroinflammation and cognitive dysfunction after surgery. Brain Behav Immun 61 365–374. [PubMed: 28089560]

Zhou H, Sun J, Zhong W, Pan X, Liu C, Cheng F, et al., 2020 Dexmedetomidine preconditioning alleviated murine liver ischemia and reperfusion injury by promoting macrophage M2 activation via PPARgamma/STAT3 signaling. Int Immunopharmacol 82 106363. [PubMed: 32145512]

Highlights

- Sepsis induces neuroinflammation and sepsis-associated encephalopathy (SAE)
- Dexmedetomidine attenuates sepsis-induce inflammation and SAE
- α2A adrenoceptor in the astrocytes may mediate dexmedetomidine neuroprotection

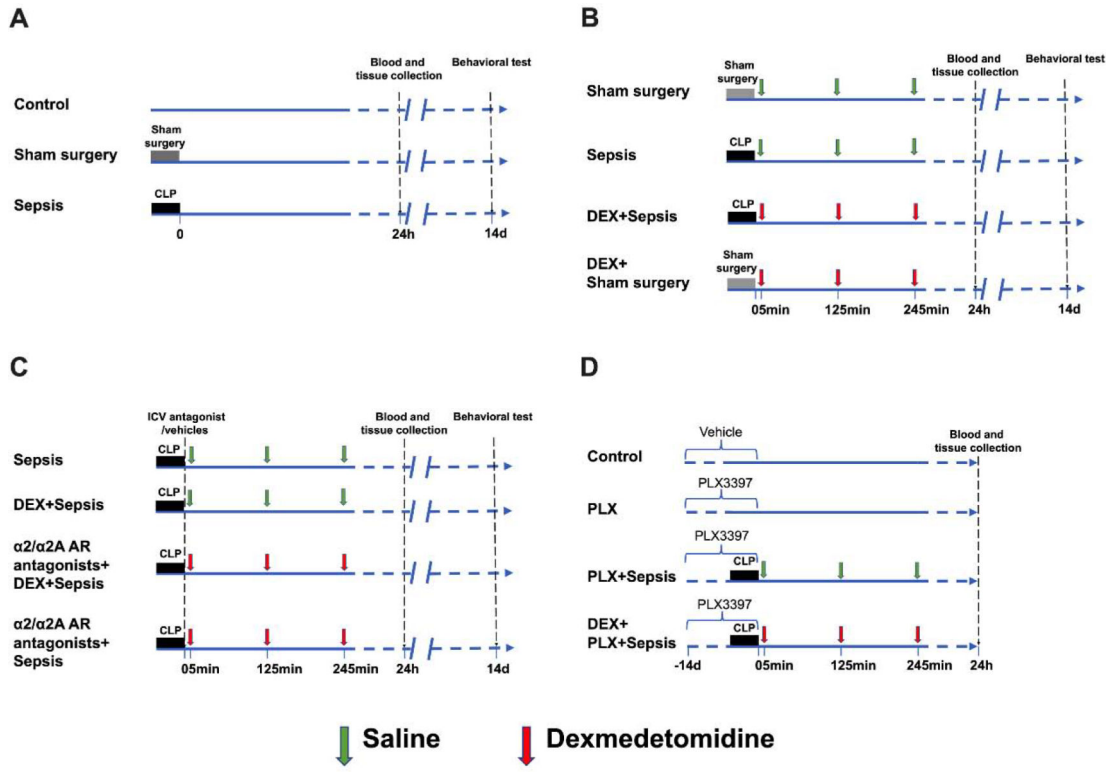

Fig. 1.

Diagram of experiments. (A) Mice were randomly allocated to 3 groups: control, sham surgery and sepsis groups. Blood and tissues were collected at 24 h after cecal ligation and puncture (CLP) or sham surgery. Fourteen days after CLP or sham surgery, Barnes maze and fear conditioning tests were used to determine the learning and memory function of mice. (B) Mice were randomly allocated to 4 groups: sham surgery, sepsis, dexmedetomidine + sham surgery, and dexmedetomidine + sepsis groups. Blood and tissues were collected at 24 h after CLP or sham surgery. Fourteen days after CLP or sham surgery, Barnes maze and fear conditioning tests were used to determine the learning and memory function of mice. (C) Mice were randomly allocated to 4 groups: sepsis, dexmedetomidine + sepsis, intracerebroventricular α2/α2A adrenoceptor antagonists + dexmedetomidine + sepsis and intracerebroventricular α2/α2A adrenoceptor antagonists + sepsis groups. The α2 adrenoceptor antagonist was atipamezole or yohimbine and α2A adrenoceptor antagonist was BRL-44408. Blood and tissues were collected at 24 h after CLP. Fourteen days after CLP or sham surgery, Barnes maze and fear conditioning tests were used to determine the learning and memory function of mice. (D) Mice were randomly allocated to 4 groups: control, PLX3397, PLX3397 + sepsis and dexmedetomidine + PLX3397 + sepsis groups. Blood and tissues were collected at 24 h after CLP. Since harvesting blood and tissues are terminal procedures, the animals for harvesting blood and tissues were a different cohort from those animals used in behavioral testing.

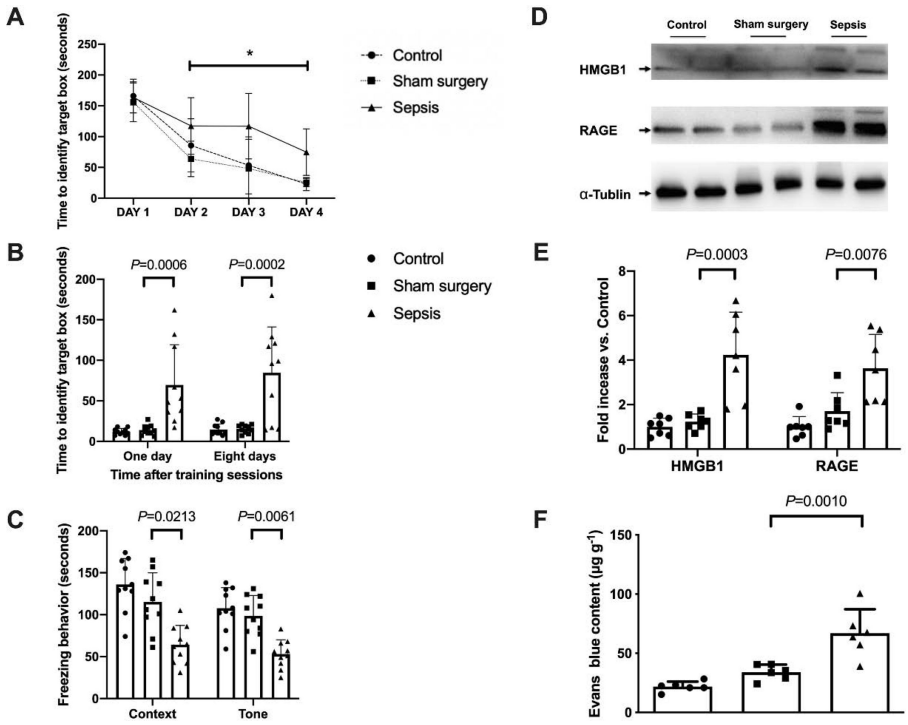

Fig. 2.

Sepsis impaired learning, memory and BBB integrity in mice. (A) Training sessions of Barnes maze. (B) Memory phase of Barnes maze. (C) Context- and tone-related fear conditioning test. (D) Representative Western blotting images of samples from the hippocampus. (E) Quantitative results of HMGB1 and RAGE in the hippocampus. (F) Quantification of Evans blue permeated into the hippocampus. All results are expressed as mean ± S.D. (n = 10 in each group for panels A to C; n = 7 in each group for Western blotting data; n = 6 in each group for Evans blue quantification data). Each animal data point in the bar graph is also presented. * $P < 0.05$ compared with the corresponding data on day 1.

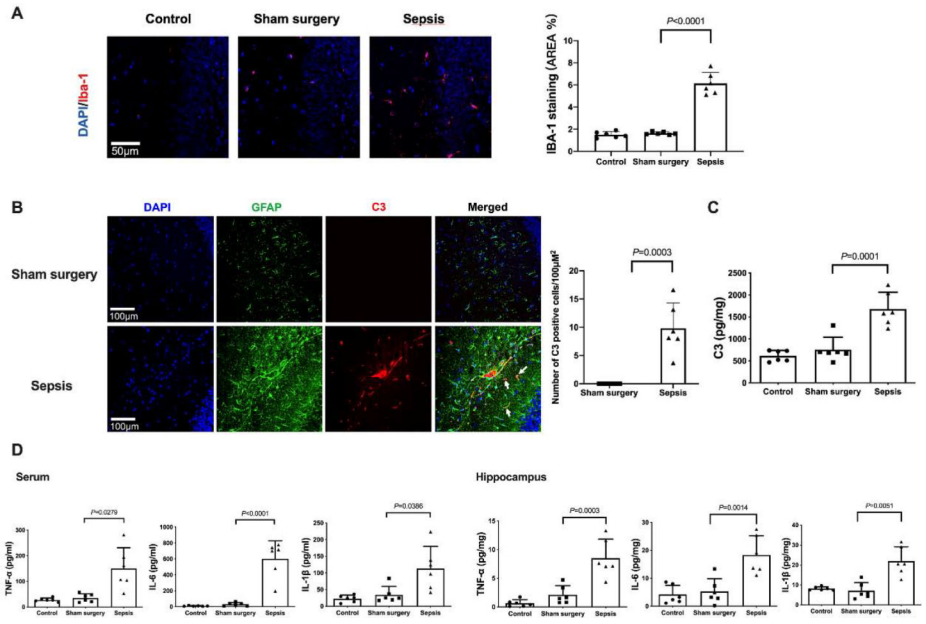

Fig. 3.

Sepsis induced systemic inflammation and neuroinflammation. (A) Left panel: representative immunofluorescent images. Scale bar = 50 μm. Right panel: quantitative results of the percentage of Iba-1 positive area in the total area of the image (whole microscopic field) in the hippocampus. (B) Left panel: representative immunofluorescent images. Scale bar = 100 μm. Arrows indicate representative co-localization of C3 staining and GFAP staining. Right panel: quantitative results of C3 positive cell density. (C) C3 concentration in the hippocampus. (D) Concentrations of TNF-α, IL-6 and IL-1β in the serum and hippocampus. All results are expressed as mean ± S.D. (n = 6 in each group). Each animal data point in the bar graph is also presented.

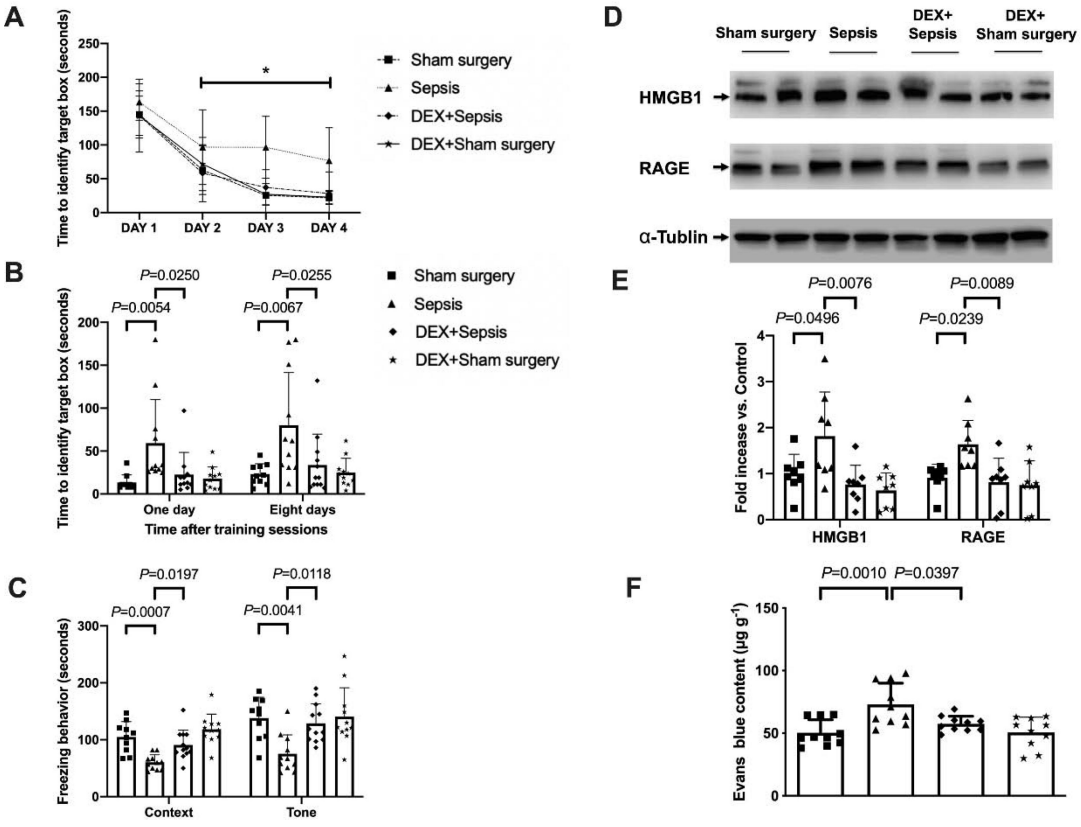

Fig. 4.

Dexmedetomidine attenuated sepsis-impaired learning, memory and BBB integrity in mice. (A) Training sessions of Barnes maze. (B) Memory phase of Barnes maze. (C) Context- and tone-related fear conditioning test. (D) Representative Western blotting images of samples from the hippocampus. (E) Quantitative results of HMGB1 and RAGE in the hippocampus. (F) Quantification of Evans blue permeated into the hippocampus. All results are expressed as mean ± S.D. (n = 10 – 12 in each group for panels A to C; n = 8 in each group for Western blotting data; n = 10 in each group for Evans blue quantification data). Each animal data point in the bar graph is also presented. * P < 0.05 compared with the corresponding data on day 1. Dex: dexmedetomidine.

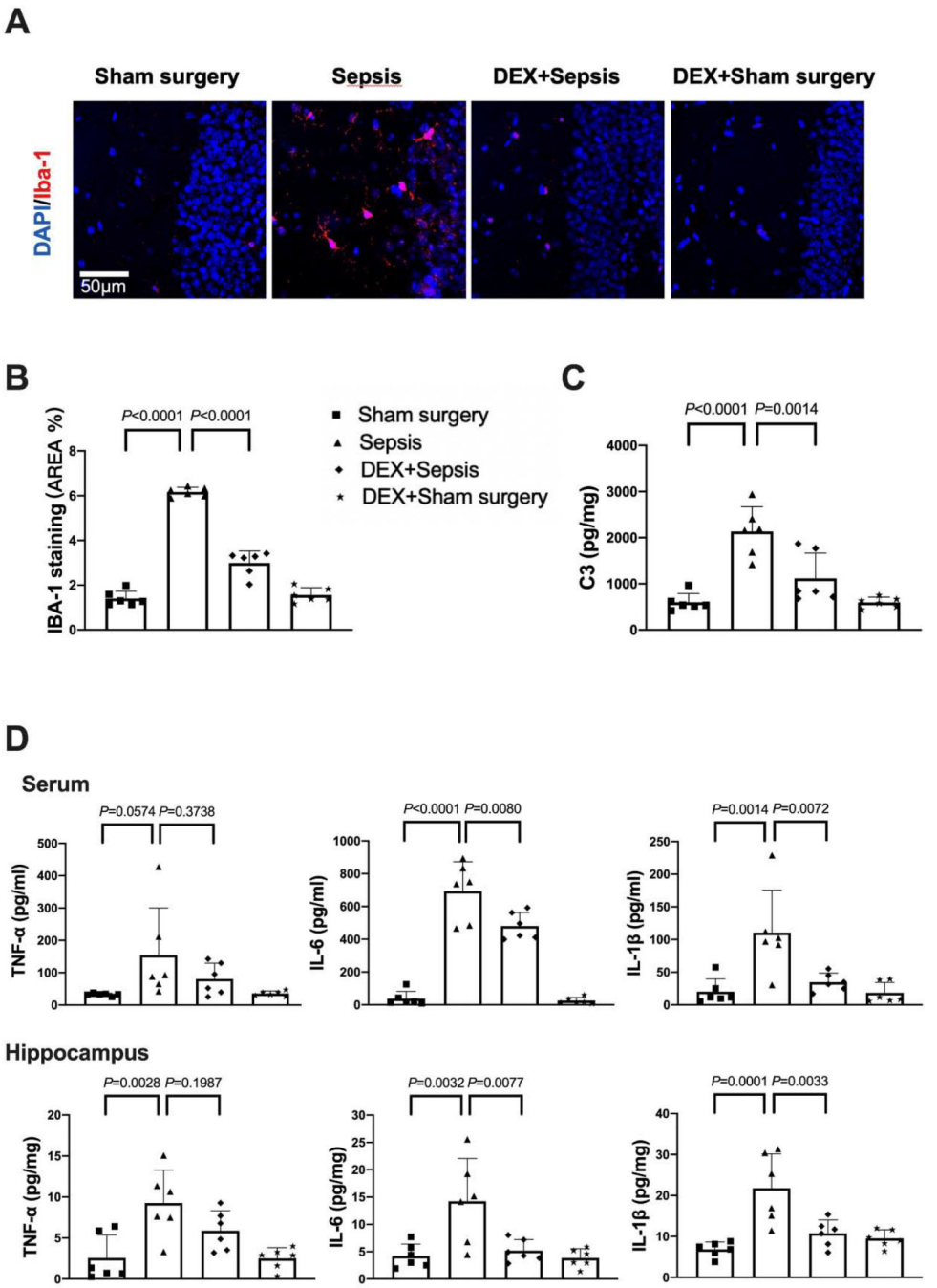

Fig. 5.

Dexmedetomidine attenuated sepsis-induced systemic inflammation and neuroinflammation. (A) Representative immunofluorescent images. Scale bar = 50 μm. (B) Quantitative results of the percentage of Iba-1 positive area in the total area of the image in the hippocampus. (C) C3 concentration in the hippocampus. (D) Concentrations of TNF-α, IL-6 and IL-1β in the serum and hippocampus. All results are expressed as mean ± S.D. (n = 6 in each group). Each animal data point in the bar graph is also presented. Dex: dexmedetomidine.

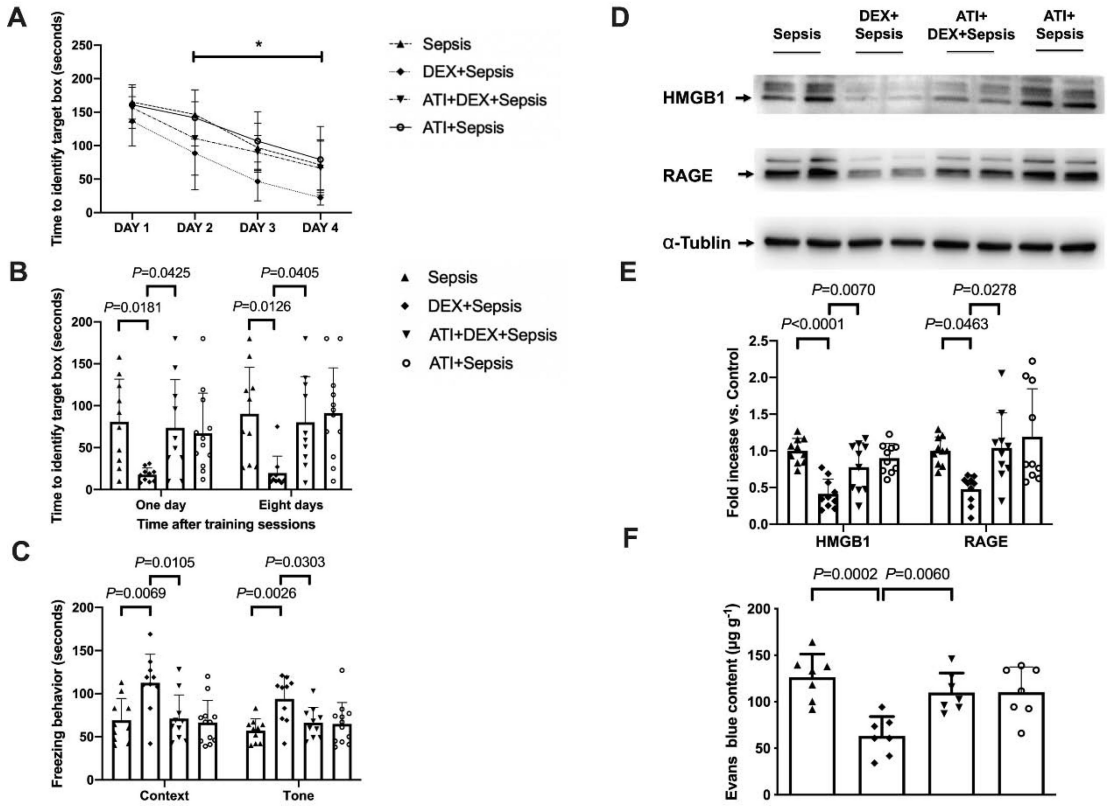

Fig. 6.

Intracerebroventricular α2 adrenoceptor antagonist (atipamezole) reduced dexmedetomidine protection on sepsis-impaired learning, memory and BBB integrity in mice. (A) Training sessions of Barnes maze. (B) Memory phase of Barnes maze. (C) Context- and tone-related fear conditioning test. (D) Representative Western blotting images of samples from the hippocampus. (E) Quantitative results of HMGB1 and RAGE in the hippocampus. (F) Quantification of Evans blue permeated into the hippocampus. All results are expressed as mean ± S.D. (n = 10 – 12 in each group for panels A to C; n = 10 in each group for Western blotting data; n = 7 in each group for Evans blue quantification data). Each data point in the bar graph is also presented. * $P < 0.05$ compared with the corresponding data on day 1. ATI: atipamezole, Dex: dexmedetomidine.

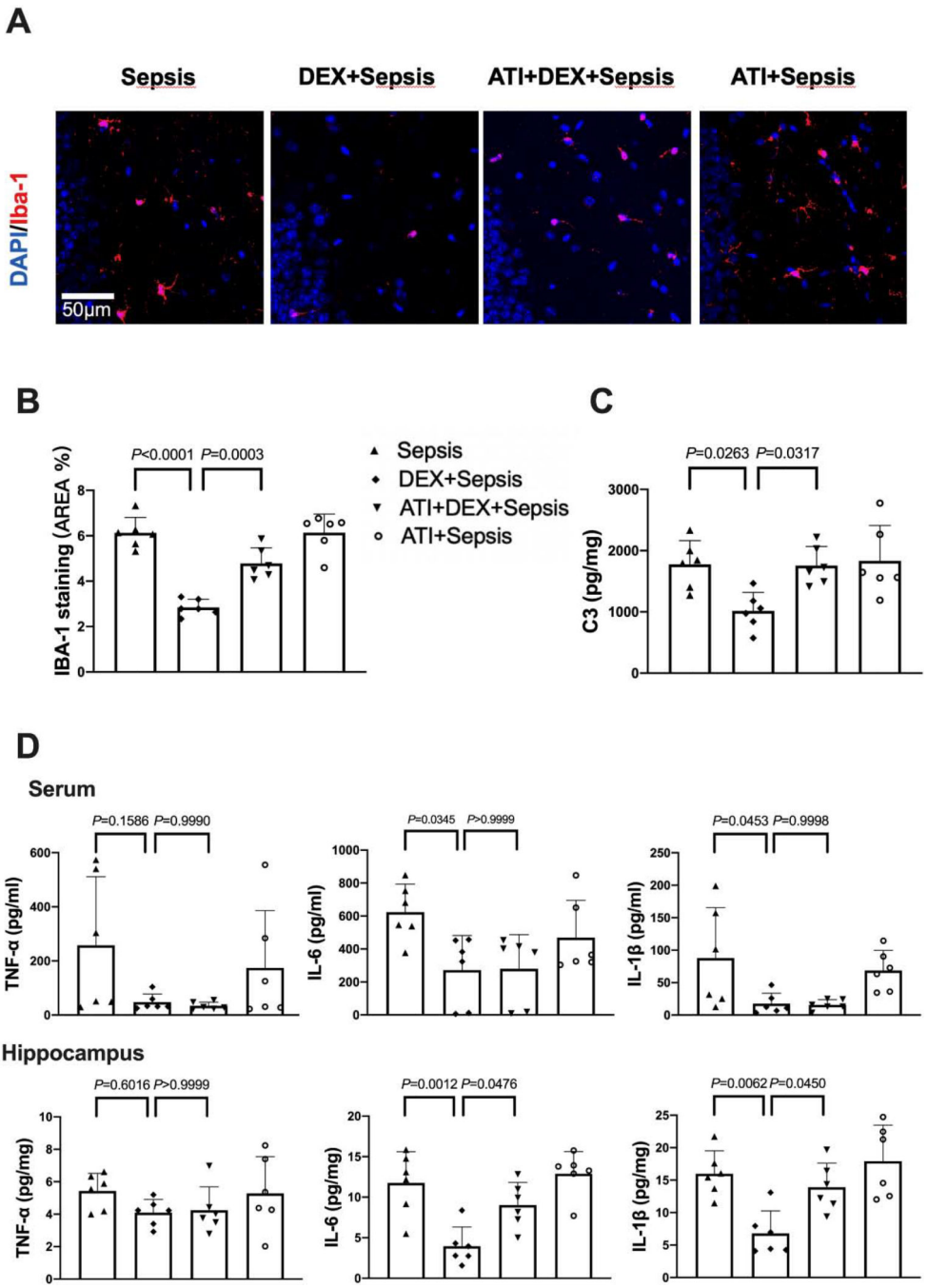

Fig. 7.

Intracerebroventricular α2 adrenoceptor antagonist (atipamezole) reduced dexmedetomidine protection on sepsis-induced systemic inflammation and neuroinflammation. (A) Representative immunofluorescent images. Scale bar = 100 μm in the upper panel and = 50 μm in the lower panel. (B) Quantitative results of the percentage of Iba-1 positive area in the total area of the image in the hippocampus. (C) C3 concentration in the hippocampus. (D) Concentrations of TNF-α, IL-6 and IL-1β in the serum and hippocampus. All results are

expressed as mean ± S.D. (n = 6 in each group). Each animal data point in the bar graph is also presented. ATI: atipamezole, Dex: dexmedetomidine.

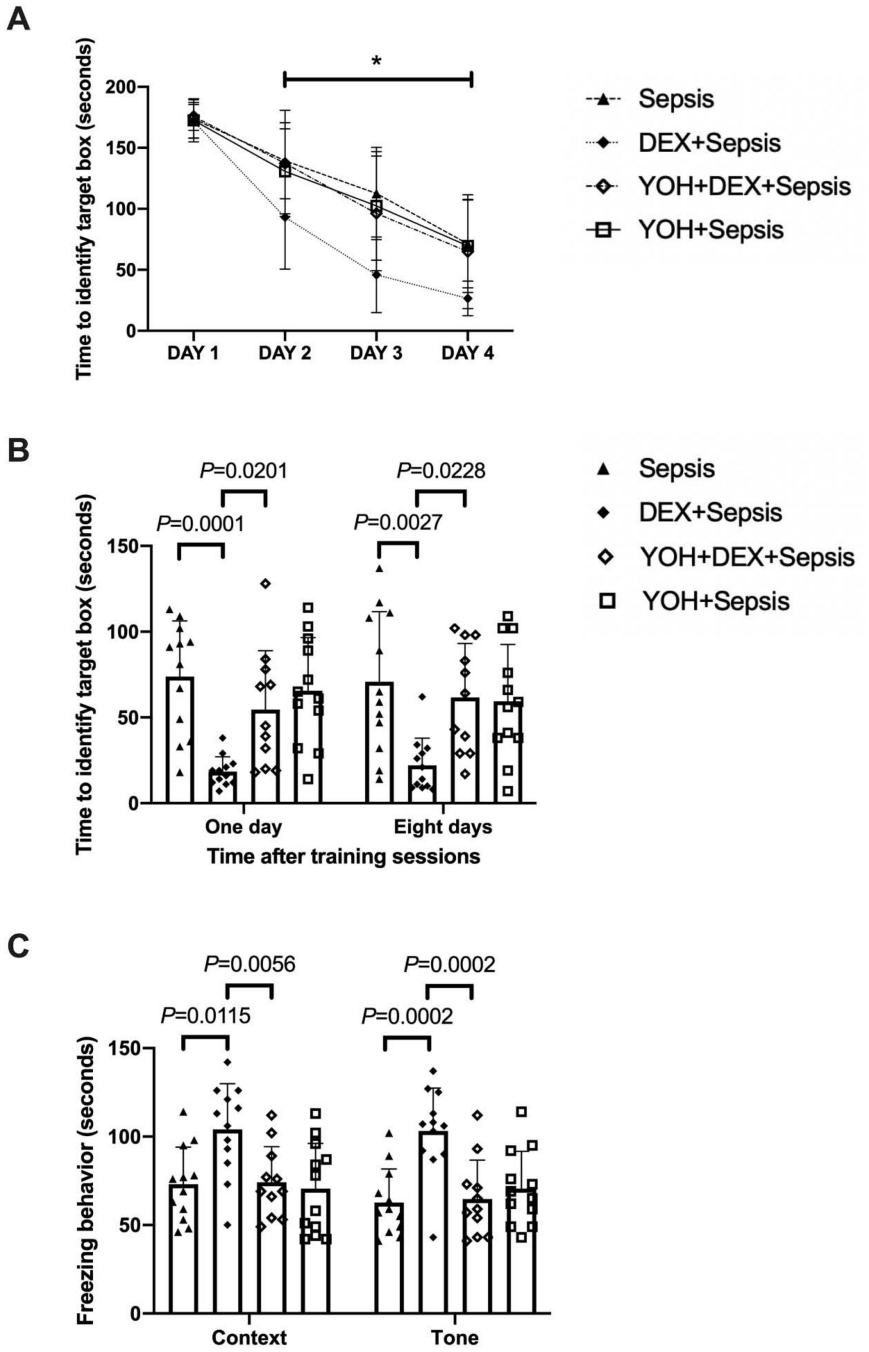

Fig. 8.

Intracerebroventricular α2 adrenoceptor antagonist (yohimbine) reduced dexmedetomidine protection on sepsis-impaired learning and memory in mice. (A) Training sessions of Barnes maze. (B) Memory phase of Barnes maze. (C) Context- and tone-related fear conditioning test. All results are expressed as mean ± S.D. (n = 11 – 12 in each group for panels A to C). Each data point in the bar graph is also presented. * $P < 0.05$ compared with the corresponding data on day 1. Dex: dexmedetomidine, Yoh: yohimbine.

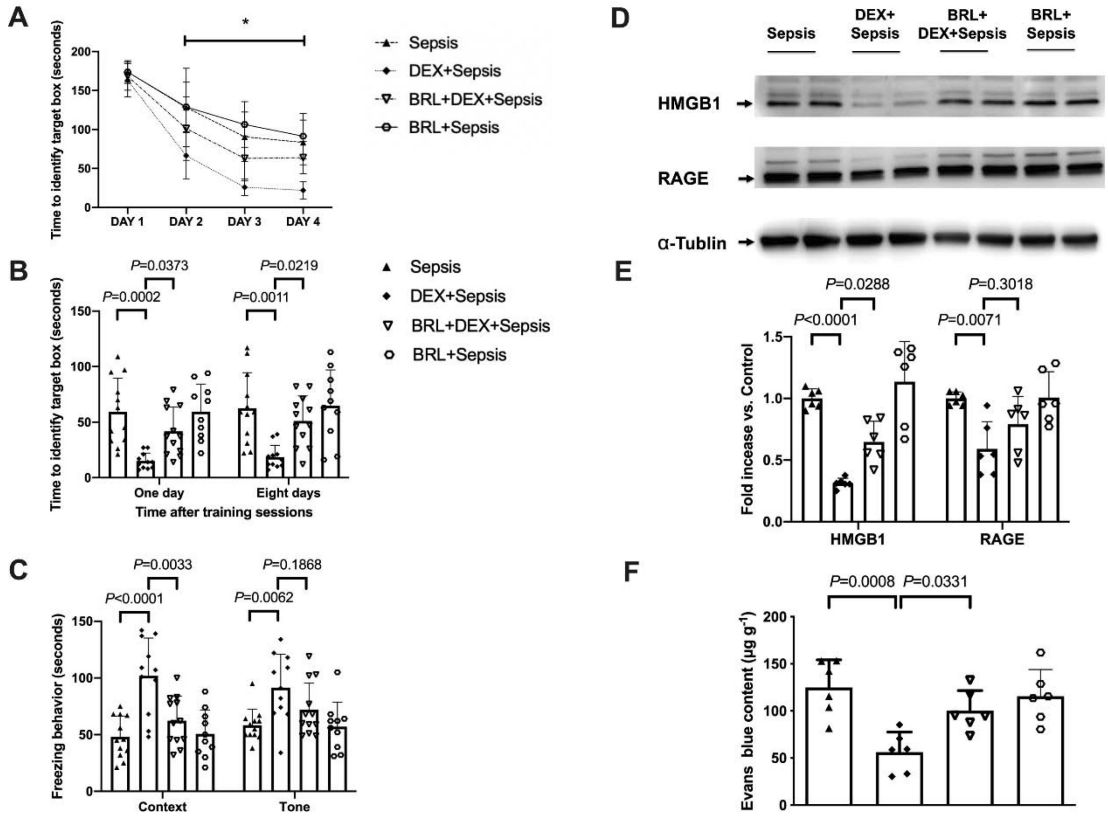

Fig. 9.

Intracerebroventricular α2A adrenoceptor antagonist (BRL-44408) reduced dexmedetomidine protection on sepsis-impaired learning, memory and BBB integrity in mice. (A) Training sessions of Barnes maze. (B) Memory phase of Barnes maze. (C) Context- and tone-related fear conditioning test. (D) Representative Western blotting images of samples from the hippocampus. (E) Quantitative results of HMGB1 and RAGE in the hippocampus. (F) Quantification of Evans blue permeated into the hippocampus. All results are expressed as mean ± S.D. (n = 10 – 12 in each group for panels A to C; n = 6 in each group for Western blotting data; n = 6 in each group for Evans blue quantification data). Each animal data point in the bar graph is also presented. * P < 0.05 compared with the corresponding data on day 1. BRL: BRL-44408, Dex: dexmedetomidine.

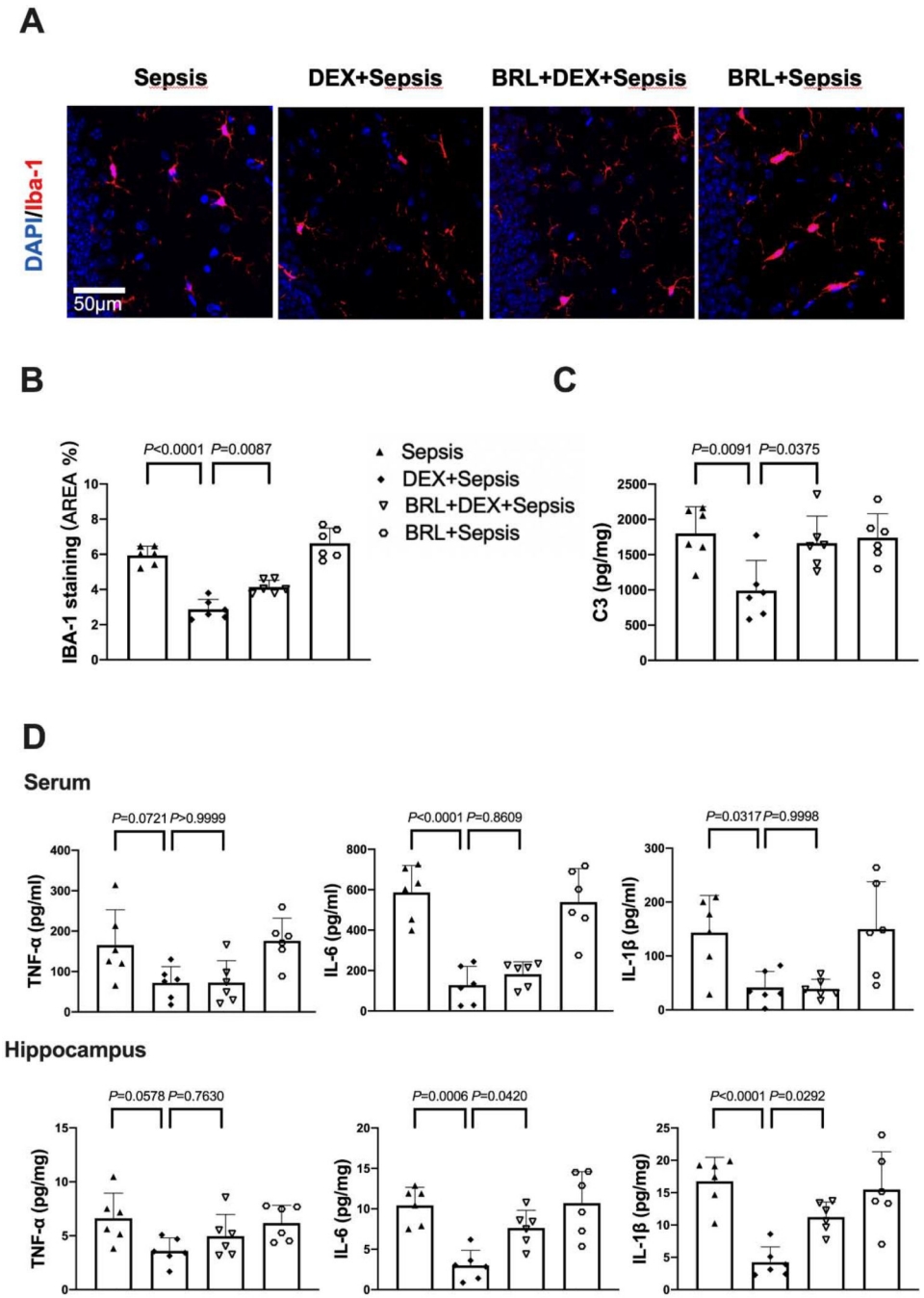

Fig. 10.

Intracerebroventricular α2A adrenoceptor antagonist (BRL-44408) reduced dexmedetomidine protection on sepsis-induced systemic inflammation and neuroinflammation. (A) Representative immunofluorescent images. Scale bar = 100 μm in the upper panel and = 50 μm in the lower panel. (B) Quantitative results of the percentage of Iba-1 positive area in the total area of the image in the hippocampus. (C) C3 concentration in the hippocampus. (D) Concentrations of TNF-α, IL-6 and IL-1β in the serum and

hippocampus. All results are expressed as mean ± S.D. (n = 6 in each group). Each animal data point in the bar graph is also presented. BRL: BRL-44408, Dex: dexmedetomidine.

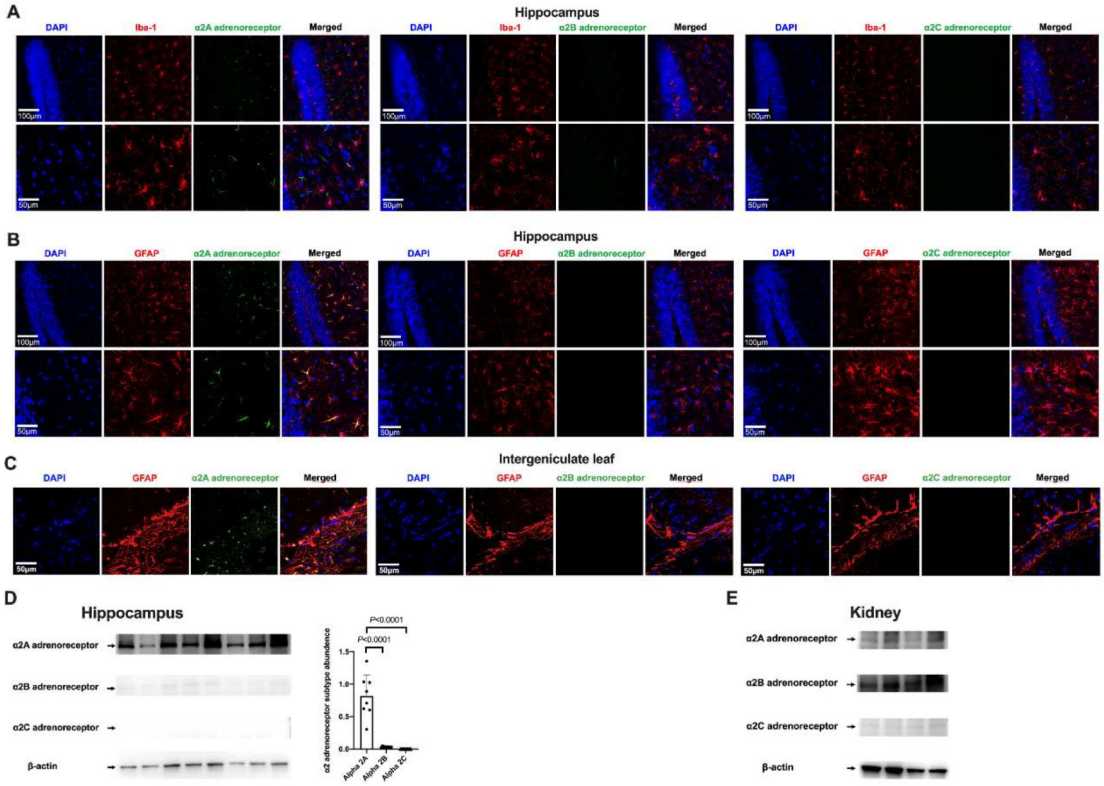

Fig. 11.

Immunofluorescent staining and Western blotting analysis of α2 adrenoceptor subtypes in the brain and kidneys. (A) Co-localization of α2 adrenoceptor subtypes with Iba-1 in the hippocampus. (B) Co-localization α2 adrenoceptor subtypes with GFAP in the hippocampus. Scale bar = 100 μm in the upper panel and = 50 μm in the lower panel for panels A and B. (C) Co-localization α2 adrenoceptor subtypes with GFAP in the intergeniculate leaf. Scale bar = 50 μm. (D) Left panel: representative Western blotting images of samples from the hippocampus. Right panel: quantitative results of HMGB1 and RAGE in the hippocampus. Results are expressed as mean ± S.D. (n = 8 in each group). Each animal data point in the bar graph is also presented. (E) Representative Western blotting images of samples from the kidneys.

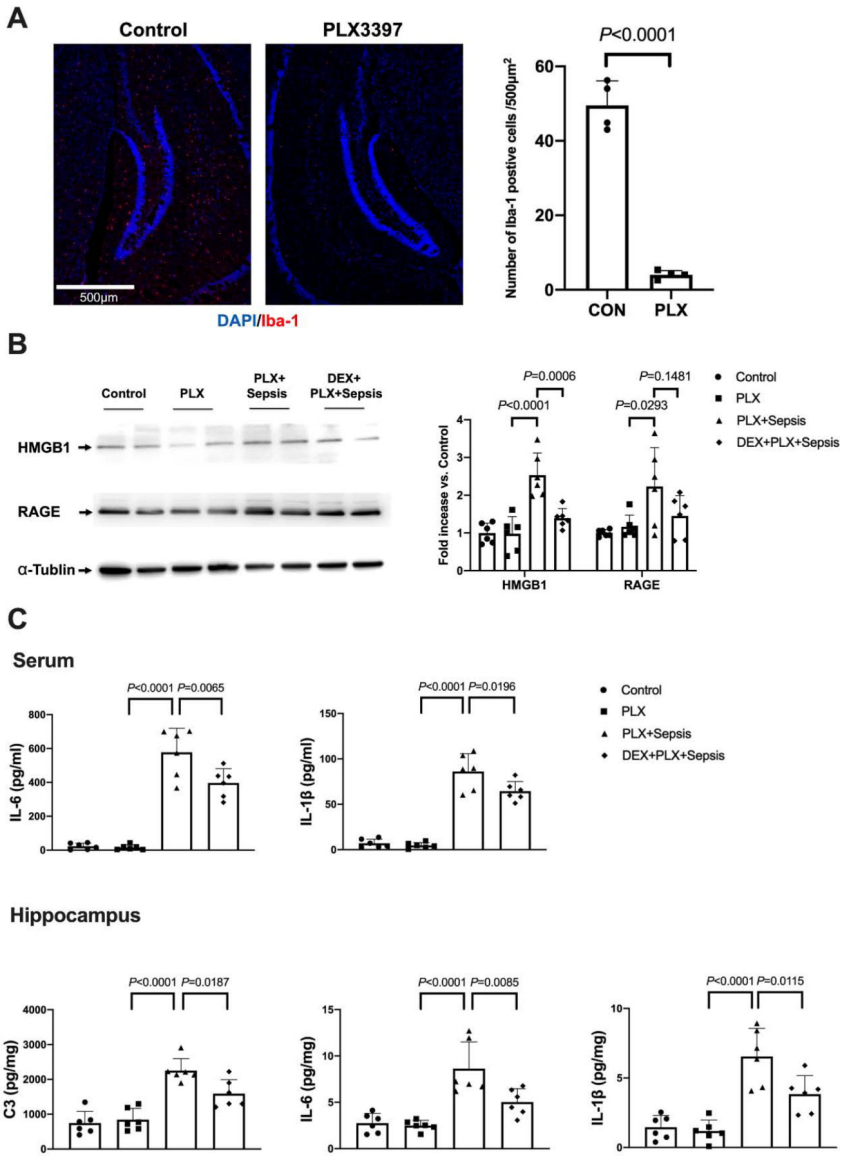

Fig. 12.

Dexmedetomidine remained to be effective to reduce systemic inflammation and neuroinflammation in septic mice depleted of microglia. (A) Presentation of microglial depletion by PLX3397. Left panel is representative images of Iba-1 immunostaining. Scale bar = 500 μm. Right panel is quantification of Iba-1 positive cells. (B) Representative Western blotting images. (C) Concentrations of IL-6 and IL-1β in the serum and concentrations of C3, IL-6 and IL-1β in the hippocampus. All results are expressed as mean ± S.D. (n = 4 for panel A; n = 6 in each group for all other panels). Each animal data point in the bar graph is also presented. PLX: PLX3397, Dex: dexmedetomidine.